View metadata, citation and similar papers at core.ac.uk

brought to you by CORE

provided by Apollo

Journal of Physics D: Applied Physics

ACCEPTED MANUSCRIPT • OPEN ACCESS

Porous Nitride Semiconductors Reviewed

To cite this article before publication: Peter Hugh Griffin *et al* 2020 *J. Phys. D: Appl. Phys.* in press https://doi.org/10.1088/1361-6463/ab9570

Manuscript version: Accepted Manuscript

Accepted Manuscript is "the version of the article accepted for publication including all changes made as a result of the peer review process, and which may also include the addition to the article by IOP Publishing of a header, an article ID, a cover sheet and/or an 'Accepted Manuscript' watermark, but excluding any other editing, typesetting or other changes made by IOP Publishing and/or its licensors"

This Accepted Manuscript is **© 2020 IOP Publishing Ltd**.

As the Version of Record of this article is going to be / has been published on a gold open access basis under a CC BY 3.0 licence, this Accepted Manuscript is available for reuse under a CC BY 3.0 licence immediately.

Everyone is permitted to use all or part of the original content in this article, provided that they adhere to all the terms of the licence https://creativecommons.org/licences/by/3.0

Although reasonable endeavours have been taken to obtain all necessary permissions from third parties to include their copyrighted content within this article, their full citation and copyright line may not be present in this Accepted Manuscript version. Before using any content from this article, please refer to the Version of Record on IOPscience once published for full citation and copyright details, as permissions may be required. All third party content is fully copyright protected and is not published on a gold open access basis under a CC BY licence, unless that is specifically stated in the figure caption in the Version of Record.

View the article online for updates and enhancements.

This content was downloaded from IP address 86.21.217.69 on 18/06/2020 at 10:03

1
2
3
4
5
6
7
8
9
10
11
12
13
14
15
16
17
18
19
20
21
22
23
24
25
26
27
28
29
30
31
32
33
34
35
36
37
38
39
40
41
42
43
44
45
46
47
48
49
50
51
52
53
54
55
56
57
58
59
60

Porous Nitride Semiconductors Reviewed

P. H. Griffin[1] and R. A. Oliver[1]

[1] Department of Materials Science & Metallurgy, University of Cambridge, 27 Charles Babbage Road, Cambridge, CB3 0FS

Abstract

Porous nitride semiconductors are a fast-developing area of study, which open up a wide range of new properties and applications, including strain free optical reflectors, chemical sensors and as a pathway to device lift-off. This article reviews the current progress in porous nitrides formed through electrochemical and photoelectrochemical methods. Using a simple electrochemical cell, pores are formed by injecting holes into the surface layer in order to oxidise the material into a soluble form and releasing nitrogen gas. The process is controlled principally by the electric field that drives the injection of holes and hence the applied potential and doping density are the key parameters for controlling pore morphology, along with how and whether illumination is used. We describe the mechanisms responsible for this process in detail and outline the trends for changing pore size and pore shape. For example, larger applied potential creates a larger electric field and hence larger pores. These methods have been used to produce a wide variety of different structures. We present a layered porous structure created by the modulation of the applied potential. Alternatively, layered structures can be produced by growing alternate doped and non-intentionally doped layers. Electrochemical etching can then create pores only in the doped layers, as they are conductive. This process can be performed by etching laterally through access trenches that expose the doped material or through the etching of dislocations to create nanopipes that allow subsurface porosity to form. This process requires no prior processing steps. We combine this method with patterning of surface protective layers to influence where the resulting pores grow. Based on these various fabrication processes, significant progress has been made towards applications of porous GaN across optoelectronics, sensing and for improving material quality.

Introduction

Nitride semiconductors are one of the most important families of semiconductor, offering a material system whose bandgap spans the entire visible spectrum through alloys of InN, GaN and AlN. These materials have allowed the blossoming of efficient LED lighting [1] and are transforming high power transistors [2]. Porous nitride semiconductors represent a new development that broadens the potential applications for the nitrides to include sensors [3,4], catalysis [5,6], and hybrid materials [7], as well as providing routes to improve the efficiency of more conventional nitride devices [8–10], improve material quality [11,12] and to create novel structures, such as membranes [13,14]. Etching nitride semiconductors via traditional wet-etching methods is notoriously difficult due to their chemical stability [15], meaning that techniques for creating new nano- and micro-structures are fairly limited. Reactive ion etching (RIE) can be used for top down etching [16,17], and KOH based solutions can be used to selectively etch certain nitride layers over others to create an undercut [18]. By bringing electrochemical etching (ECE) techniques into play, however, there is a much wider array of possible morphologies that can be fabricated.

Forming porous semiconductors via ECE is not new; the most widely studied porous semiconductor is porous Si, first fabricated in the 1950s [19]. It did not receive much interest, however until 1990 when Leigh Canham demonstrated luminescence from porous Si [20], which led to much excitement around the possibility of all Si photonic devices. Despite the excitement, commercial development of porous Si photonics has been prevented by the instability of the luminescence [21] and the material's high resistivity [22,23] due to Si's readiness to oxidise and high sensitivity to surface states. The opportunities arising from porous nitrides are not limited by these constraints, as they are highly inert and properties are much less affected by surface states. While there are many alternative ways to make porous nitrides [24–27], this review will focus on the large body of work using ECE and photo-electrochemical etching (PECE). This presents a versatile system, allowing the formation of a wide range of pore morphologies for surface and subsurface pores with wide applications to industrial

Accepted Manuscript

development. The review briefly describes the experimental set-up for forming pores in the nitrides using electrochemical methods. It then goes on to give a detailed analysis of the mechanisms responsible for pore formation and how these can be related to the observed pore morphology through the depletion model. The focus of this section is to give the reader an understanding of the mechanisms that drive the pore formation process and affect the resulting morphology, rather than to provide a comprehensive collection of experimental recipes. Next it describes the wide range of porous structures that have been demonstrated in the nitrides, including in nitrides other than GaN. Finally it describes the opportunities and challenges of the emerging applications.

Methods and Mechanisms of Electrochemical Pore Formation

Experimental Set-up

ECE and PECE of GaN has been performed with wide ranging parameters to form porous structures with various morphologies. The basic set-up is the same for all of these and is shown in Figure 1. This consists of:

- A nitride based sample to be porosified, connected as the anode;
- An inert counter electrode, connected as the cathode, usually platinum;
- An electrolyte, forming an ionic conduction path between the electrodes;
- An applied potential between the anode and cathode from a voltage or current source;
- In the case of photo-electrochemical etching (PECE) the sample is also illuminated, normally using a high energy UV lamp.

Within this basic set-up there are wide choices to be made of growth structure, electrolyte, applied potential and illumination power and wavelength. There are also differences in the physical set-up, such as the inclusion of a known reference electrode (e.g. Ag/AgCl) or the use of a stirrer or pump to create electrolyte flow.

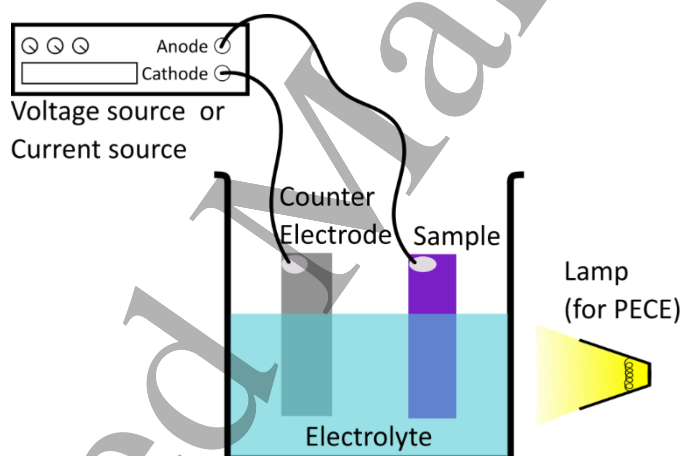

Figure 1: A schematic illustration of the basic electrochemical set-up for forming porous GaN.

The Electrochemical Process

PECE of GaN was first used for electropolishing, i.e. removing material completely rather than just porosifying it [28]. In that work, the applied potential was very low and without illumination no etching was observed. This could be best described as electrically enhanced photochemical etching, as the reaction is driven by the incident light and the role of the potential is simply to remove the photo-generated carriers. The authors proposed a mechanism for the process based on prior work on GaAs that the photo-injected holes assist the oxidation of Ga. The oxidation of GaN is an electrochemical reaction, driven by holes and can be shown as [29]:

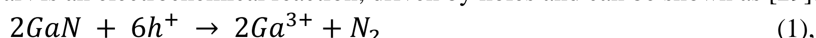

$$2GaN + 6h^{+} \rightarrow 2Ga^{3+} + N_2 \quad (1),$$

The Ga^{3+} ions can then dissolve in the electrolyte. This is now generally accepted as the appropriate mechanism for electrochemical etching of nitrides in both ECE and PECE [30,31], although some work specifies that Ga_2O_3 is formed, which can then be dissolved in the electrolyte [32]. This fits with the finding that when the same process is performed with pure water as the electrolyte, the surface is oxidised, but the oxide is not dissolved, so pores are not created [33].

Accepted Manuscript

1
2
3
4
5
6
7
8
9
10
11
12
13
14
15
16
17
18
19
20
21
22
23
24
25
26
27
28
29
30
31
32
33
34
35
36
37
38
39
40
41
42
43
44
45
46
47
48
49
50
51
52
53
54
55
56
57
58
59
60

Equation 1 shows that the process is driven by free holes. In the case of PECE, the incident light creates electron-hole pairs and the photogenerated holes are swept to the nitride/electrolyte interface by the applied electric field, where they drive the etching reaction [34]. In ECE there are no photogenerated carriers, but holes can be created in an n-type semiconductor in two ways: Zener tunnelling or impact ionization. In Zener tunnelling the band bending resulting from the applied negative potential at the electrolyte interface is large enough that the valence band at the interface reaches a higher energy than the conduction band in the bulk. This allows electrons to tunnel from the interface valence band into the bulk conduction band, leaving behind a free hole. This is only possible with high doping, such that the space-charge region (SCR) is thin enough to allow tunnelling. Impact ionization occurs under an even larger electric field. In this case a highly energetic conduction band electron creates an electron hole pair by colliding with a valence band electron and losing its kinetic energy. This requires carriers to be accelerated by the electric field over a large enough distance to gain sufficient kinetic energy. Hence a large SCR is required, which occurs at low doping density. Assessment of the potentials and doping density at which pores are formed in GaN suggests that Zener tunnelling is most often the significant process [29,35], although avalanche breakdown could become significant at higher potentials and have an impact on the mechanism and morphology [36]. One model describing pore formation in III-V semiconductors more generally is the current burst model. In this situation avalanche breakdown occurs around some inhomogeneity and causes a large supply of holes that drives an oxidation reaction. The oxide that forms then quenches the reaction by reducing the electric field at that point. The oxide is steadily dissolved by a chemical process until it becomes thin enough for another burst to occur [37]. This leads to characteristic oscillations in the width of the pores. The current burst model has been presented in detail as one mechanism for pore formation in silicon [38] and the oscillations have been observed in the formation of surface pores in GaN [31]. The requirement of an electric field at the nitride/electrolyte interface means that both ECE and PECE are conductivity-selective etching methods. If the material is not conductive enough then there will not be an electric field at the interface, holes will not be injected into the surface and the material will not etch. This means that NID layers can be used as etch stops. This is shown in the cross-sectional SEM image of Figure 2. Layers of Si-doped and NID GaN are grown in an alternating structure and the edge is exposed by creating trenches, using inductively coupled plasma reactive-ion etching (ICP-RIE). Through ECE the Si-doped GaN is transformed to porous GaN, which creates a highly reflective distributed Bragg reflector (DBR). The NID material forms an effective etch stop, as the applied electric field between this material and the electrolyte is zero, so there is nothing to generate the free holes necessary to drive the oxidation reaction. Almost all reported porous nitride materials are n-type doped due to the requirement for reasonably high conductivity and the challenge of effective p-type nitride doping. Porosity has been created at the surface of p-type GaN using PECE [33,39], as well as a novel approach using alternating current [40]. This approach is a PECE based method in which the material is oxidised during the positive half cycle of the applied current, by the same chemical reaction given in Equation **1**, while electrons are removed from the surface during the negative half cycle, in order to prevent the accumulation of surface electrons, which would tend to inhibit the etching process [41].

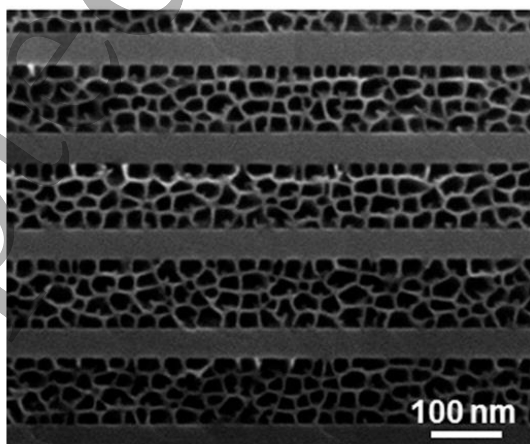

Figure 2: Cross-sectional SEM image of a GaN/porous GaN DBR. The porous layers are separated by solid GaN layers, which is the NID material. Reproduced with permission from [8]. Copyright 2015 American Chemical Society.

Accepted Manuscript

1
2
3
4
5
6
7
8
9
10
11
12
13
14
15
16
17
18
19
20
21
22
23
24
25
26
27
28
29
30
31
32
33
34
35
36
37
38
39
40
41
42
43
44
45
46
47
48
49
50
51
52
53
54
55
56
57
58
59
60

The Depletion Model of Pore Formation

The doping density and the applied potential are the two most influential factors in controlling pore formation and their morphology, as these are the ways of changing the applied electric field. Figure 3 shows a phase diagram to illustrate this for the ECE of GaN [31]. When the applied potential and doping concentration are low there is no etching, as the electric field is not large enough to inject holes into the surface GaN to oxidise it. Increasing the potential and/or the doping concentration increases the electric field applied at the GaN/electrolyte interface. At some point, the electric field will be large enough to cause hole injection at certain "hotspots" and etching will begin to form pores. Increasing potential and/or doping density further allows the electric field to completely etch the doped layer to cause electropolishing. Within the central region of Figure 3 where porous etching is achievable, there is a range of achievable morphologies. Pore size can be controlled by varying the applied potential for a given doping density or vice versa. At a high potential, near the electropolishing regime, pores are large, whereas at low potential, near the no etching regime, pores are small [35]. Figure 4 shows three cross-sectional SEM images, which illustrate the variation of pore morphology with potential and doping density for a doped GaN layer etched laterally in a nitric acid electrolyte. The leftmost SEM image shows pores formed close to the electropolishing regime with $N_D = 1 \times 10^{20}$ cm^{-3} and a large potential (in this case 3 V. The topmost porous layer in the middle SEM image has the same N_D, but a lower applied potential and this produces smaller, denser pores. The lower porous layer in this image has slightly smaller pores again, due to a lower doping density of $N_D = 7 \times 10^{19}$ cm^{-3}, while the porous layers in the rightmost image have even lower values ($N_D = 3 \times 10^{19}$ cm^{-3} and $N_D = 1 \times 10^{19}$ cm^{-3} for the top and bottom layers respectively) and is etched at the lowest potential. This leads to layers of sparse, small pores.

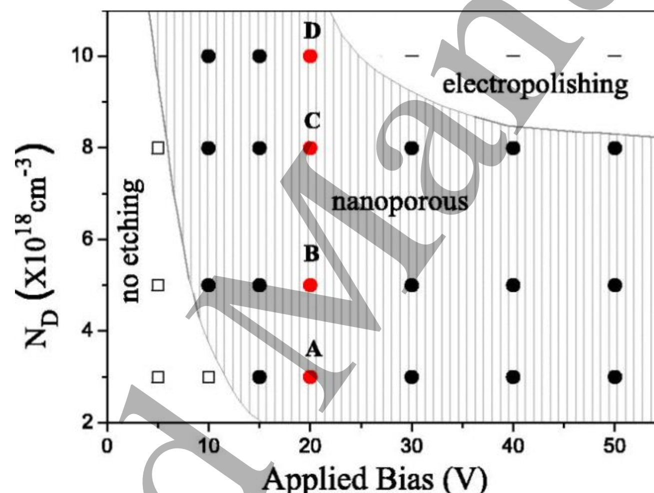

Figure 3: Phase diagram showing how the dual factors of potential and doping density control the etching process, showing the no etching regime, where the electric field is too low (squares), the electropolishing regime where all doped material is removed (horizontal lines), and between these two the "nanoporous" regime, where pores are formed (circles). The red annotations are not referred to within this review article. Reprinted from [31], with the permission of AIP Publishing.

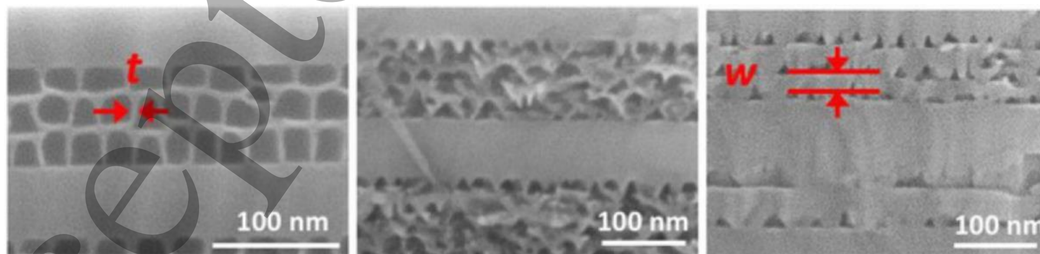

Figure 4: Cross-sectional SEM images for three samples etched laterally in Nitric acid, showing pores close to the electropolishing regime (left) to close to the onset of etching (right). Left: $N_D = 1 \times 10^{20}$ cm^{-3}/undoped GaN alternating layers with a potential of around 3 V. Middle: $N_D = 1 \times 10^{20}$ cm^{-3}/undoped GaN/$N_D = 7 \times 10^{19}$ cm^{-3} layers from top to bottom, with a potential of around 2 V. Right: $N_D = 3 \times 10^{19}$ cm^{-3}/undoped GaN/$N_D = 1 \times 10^{19}$ cm^{-3} layers from top to bottom, with a potential of around 1 V. The red annotations are not referred to within this review article. Reprinted from [35].

Accepted Manuscript

1
2
3
4
5
6
7
8
9
10
11
12
13
14
15
16
17
18
19
20
21
22
23
24
25
26
27
28
29
30
31
32
33
34
35
36
37
38
39
40
41
42
43
44
45
46
47
48
49
50
51
52
53
54
55
56
57
58
59
60

The morphology of pores formed under different etching conditions can be understood through a depletion model [31]. When a positive potential is applied to an n-doped planar nitride semiconductor relative to an electrolyte, the electric field will create band bending at the surface, causing a depletion region to grow and if the potential is large enough, forming an inversion layer. Injected holes can then drive the oxidation of GaN by the electrochemical process shown in equation 1, which removes material. For a planar surface, the size of the electric field at the nitride surface will be defined by the potential across the depletion region and its width:

$$E_{Depl} = \frac{V_{Depl}}{W_{Depl}} \quad (2),$$

where E_{Depl} is the electric field across the depletion region, V_{Depl} is the potential dropped across it and W_{Depl} is the width of the depletion region. It is generally assumed that V_{Depl} will be a significant proportion of the applied potential, as the depletion region is highly resistive compared to the bulk semiconductor and the electrolyte [42]. Some work has suggested that the voltage drop along a GaN electrode is significant, this will depend strongly on the particular doping density, layer thickness and sample length [43]. To derive W_{Depl} we can use the derivation of the depletion width for a reverse biased p+n junction (see [44] or similar textbook), where we assume the space charge region in the electrolyte is negligible:

$$W_{Depl} = \sqrt{\frac{2\epsilon_r \epsilon_0 V_{Depl}}{qN_D}} \quad (3),$$

where ϵ_r is the relative permittivity of the semiconductor, ϵ_0 is the permittivity of free space, q the fundamental charge of an electron and N_D is the donor doping density of the semiconductor. Combining equations 2 and 3 gives:

$$E_{Depl} = \sqrt{\frac{q}{2\epsilon_r \epsilon_0}} \sqrt{V_{Depl} N_D} \quad (4),$$

Thus, E_{Depl} and W_{Depl} are both proportional to the root of V_{Depl}, while E_{Depl} is also proportional to the root of N_D, but W_{Depl} is proportional to the inverse of the root of N_D. Following [35], we can define a critical electric field, E_{Crit} above which material will be etched. Approximating the pores as circular in a 2D model, the thickness of the walls between pores, t, is then given by:

$$t = \frac{2\epsilon_r \epsilon_0 E_{Crit}}{qN_D} \quad (5),$$

This indicates that the pore wall thickness is independent of voltage, but inversely proportional to N_D. This would suggest that the pore walls become thicker with a large decrease in N_D, as has been shown experimentally [31]. As N_D decreases, a larger potential is required to achieve E_{Crit}. Continuing with the 2D circular pore model from [35], the electric field at distance r from the pore centre is given by:

$$E(r) = \frac{1}{2\pi r \epsilon_r \epsilon_0}\left[qN_D \pi (r^2 - r_0^2) + Q\right] \quad (6),$$

where r_0 is the internal radius of the pore and Q is the total charge in the anion layer. The point at which the pore stops growing in size will be when $E(r_0) = -E_{Crit}$. Using equation 6, this gives:

$$-E_{Crit} = \frac{Q}{2\pi r_0 \epsilon_r \epsilon_0} \quad (7),$$

which can be rearranged as:

$$r_0 = \frac{-Q}{2\pi \epsilon_r \epsilon_0 E_{Crit}} \quad (8),$$

Q, the total charge in the anion layer, must balance the total charge in the depletion layer, which is given by:

$$Q = \sqrt{2q\epsilon_r \epsilon_0 V_{Depl} N_D} \quad (9),$$

Therefore, for a given N_D increasing the potential will increase pore size. At large N_D, the threshold potentials required to create pores and to induce electropolishing are lower. This simple 2D analysis can therefore explain the observed morphology of pores.

The growth direction of pores formed through anodic porosification can generally be described as either crystallographically or current-line orientated [37]. No influence of crystallography on the pore growth direction has yet been observed in porous GaN [29]. Comparisons of N-polar and Ga-polar material show no significant difference after PECE [45], while pores have been formed in c-plane grown GaN by etching in various crystallographic directions and no differences have been reported between them. What's more, very similar structures have been achieved in both m-plane and a-plane grown GaN [9,46]. Instead, the pore direction can be characterised as following the flow of current and therefore perpendicular to equipotential surfaces [37]. This orientation is disrupted in the case of PECE, where the illumination creates extra holes and can change the morphology [34].

Accepted Manuscript

1
2
3
4
5
6
7
8
9
10
11
12
13
14
15
16
17
18
19
20
21
22
23
24
25
26
27
28
29
30
31
32
33
34
35
36
37
38
39
40
41
42
43
44
45
46
47
48
49
50
51
52
53
54
55
56
57
58
59
60

Pore Formation and Interaction

The data shown so far has been of pores formed laterally in doped GaN layers exposed to the electrolyte via scribed trenches. Pores can also be formed vertically in doped surface layers and this shows the same trend of decreasing pore wall thickness with increasing doping density, but shows decreasing pore size with increasing doping density. This has been shown by Chen *et al.* who found the pore wall thickness reduced from around 110 nm to around 15 nm, while the pore diameter reduced from around 65 nm to around 10 nm observed for doping density varied from 3×10^{18} cm^{-3} to 1.2×10^{19} cm^{-3} [31]. This is due to the initiation of pores and the interaction between them. For a given potential the density of pore initiation points will be larger for a higher doping density, as this reduces W_{Depl} and increases the electric field, allowing more points on the surface to reach the critical electric field. This is supported by the plan-view SEM images of Figure 5, where the density of pores increases with N_D. This can also be seen in the cross-sectional SEM images of Figure 5b-d, but N_D and the potential are changed simultaneously between these samples and as a higher potential increases the electric field too, this is less straightforward to interpret [29]. Around each pore there will exist a depletion region and as the pores grow the depletion regions of adjacent pores will meet, which reduces the electric field at the interface with the electrolyte [47]. A higher density of pores means that pores cannot grow as wide before they are inhibited by adjacent pores. This also affects the morphology of pores, which can range from highly branched (Figure 5a) to vertically aligned (Figure 5d), which is controlled by the relative lengths of the depletion region (W_{Depl}) and the distance between adjacent pores (d_{pore}). Where $d_{pore} > 2W_{Depl}$ then the material between the pores can support a current, which allows the pores to grow wider and branches can split off into the space between pores. Where $d_{pore} < W_{Depl}$ then the thin region of material between the pores is fully depleted, meaning that pores can only grow vertically and the pores are well-aligned [31]. Once initial etch pits have formed then both the density of etch pits and the curvature of the pit will have an influence on subsequent pore growth. At a curved surface with a radius of curvature, $r \ll W_{Depl}$ then the electric field is enhanced and is given by [29]:

$$E_{Depl} = {}^{V_{Depl}}/_{r} \qquad (10),$$

This acts to concentrate ECE at the pore tip, which is why pores can be formed, rather than etching away layers of material completely.

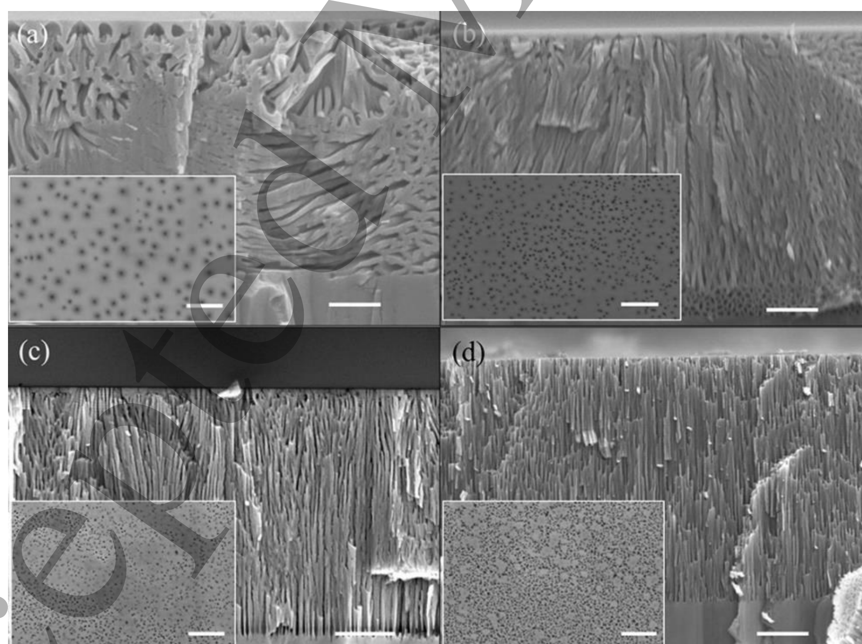

Figure 5: Cross-sectional and plan-view (inset) SEM images of porous GaN with varied N_D, anodised in 25% HF at 20 V. (a) $N_D = 3\times10^{18}$ cm^{-3}, (b) $N_D = 5\times10^{18}$ cm^{-3}, (c) $N_D = 8\times10^{18}$ cm^{-3}, (d) $N_D = 1.2\times10^{19}$ cm^{-3}. Scale bars are 500 nm. Reprinted from [31], with the permission of AIP Publishing.

Accepted Manuscript

1
2
3
4
5
6
7
8
9
10
11
12
13
14
15
16
17
18
19
20
21
22
23
24
25
26
27
28
29
30
31
32
33
34
35
36
37
38
39
40
41
42
43
44
45
46
47
48
49
50
51
52
53
54
55
56
57
58
59
60

Influence of Electrolyte

The electrolyte has two main roles that it must fulfil for ECE or PECE to occur. Firstly, it must provide a conductive path to complete the electrolytic circuit and allow an electric field at the nitride/electrolyte interface to provide the continuous supply of holes. Secondly, it must be able to prevent the formation of solid oxides forming and passivating the surface. In forming porous silicon by anodization, this requires HF based electrolytes, in order to dissolve SiO_2 [20], but a wide variety of electrolytes have been used to create porous nitride structures via ECE or PECE including both acids, such as sulphuric acid [29], HF [31] and oxalic acid [48] as well as bases, such as NaOH [32] and KOH [49]. The pH of the electrolyte has been suggested to influence the resulting pore morphology in PECE due to the relative negative charge of some dislocation centres [50]. This changes the rates of gallium oxide etching by H^+ ions and OH^- ions, with acidic electrolytes preferentially targeting dislocations and basic ones targeting the more positive regions away from dislocations, leaving dislocations un-etched. The pH can also have an influence when etching binary alloys, as different metal oxide compounds etch preferentially in different pH, which can result in an insoluble oxide film being formed [51].

The influence of electrolyte concentration has also been studied. The conventional assumption is that the semiconductor depletion region is much thicker than the thickness of the space charge region of the electrolyte , which can therefore be neglected [42] and indeed it has been suggested that electrolyte concentration for ECE of GaN in oxalic acid does not influence the observed pore morphology [52]. However, a more detailed study of electrolyte concentration of ECE in HF finds that increasing concentration (from 10% to just under 35 % by volume) reduces pore diameter (from around 40 nm to around 20 nm, increases pore wall thickness from around 20 nm to around 60 nm and changes the threshold potential necessary for the onset of porosification (from around 10 V to around 5) and electropolishing (from around 15 V to around 40 V) [31]. These numbers are likely to depend on other experimental conditions, such as the N_D of the material and are provided only as a guide. This work suggests that, at low potential, increasing concentration decreases the voltage drop in the electrolyte, which lowers the necessary potential to create pores. At high applied potential, the assumption of all the potential being dropped across the semiconductor depletion region will be more accurate, but a high electrolyte concentration will increase the chemical dissolution rate of the oxide. This reduces the rate of oxide build-up and increases the potential needed to achieve electropolishing. Although applied potential and doping density are the main parameters for controlling pore formation, choice of electrolyte pH and concentration can also be used to tune pore morphology to some extent.

Structures

As we have seen, forming porous nitrides relies on creating an electric field between the material and a suitable electrolyte. For porous GaN to be utilised in devices it is important to be able to control which regions of a structure porosify and to protect certain regions from etching. This can be done by controlling the electric field, the flow of the electrolyte and in the case of PECE the illumination. This section details methods for doing this and reviews the range of structures that have been demonstrated.

The simplest porous GaN structure is where a porous layer is formed at the surface. This can be achieved with a surface layer of doped nitride semiconductor, such that the pores initiate at the surface and grow vertically into the structure [47]. An etch stop of un-doped material can be used to control the thickness of the porous layer, else the etch duration can be controlled to terminate the reaction and the methods described above can be used to control pore morphology. In fact, quite complicated structures can be created with single doped layers, by changing the etch conditions during the reaction. In particular, modulation of the applied potential can create layers of different porosity, as is well established in porous silicon [53,54]. We have demonstrated this by applying the periodic potential profile shown in Figure 6a to a sample with a 2 μm thick n-doped layer with N_D~$5\times10^{18}cm^{-3}$ using the ECE set-up described in [9]. The potential was alternated between 8 V and 14 V holding each one for 200 and 100 seconds respectively. The current trace can be correlated with the morphology shown in the cross-sectional SEM image of Figure 6b. Initially, the current ramps up slowly and a thin, low porosity interface layer can be seen at the top surface. When the potential switches to 14 V there is a large transient before the current rises sharply, corresponding to the first highly porous layer. The potential is switched back to 8 V while the current is still rising and the current then settles to 0.4 mA. This pattern repeats twice more, but when the current switches to 8 V for the fourth time (15 minutes), the current is much lower, as there is no material left to etch. This creates a structure with a periodic variation in porosity. This method works because the electric field is concentrated at the pore tip and the potential is being carried along the un-etched

Accepted Manuscript

1 2 3 4 5 6 7 8 9 10 11 12 13 14 15 16 17 18 19 20 21 22 23 24 25 26 27 28 29 30 31 32 33 34 35 36 37 38 39 40 41 42 43 44 45 46 47 48 49 50 51 52 53 54 55 56 57 58 59 60

material, from below. This means that once material has become porous, it will not be etched any further, even upon increasing the applied potential. By varying the potentials and the timing of the applied potential a wide variety of morphologies could be achieved, but careful calibration of the settling time when switching is required. Using higher doped material may help to achieve sharper boundaries between layers, as has been found with porous silicon [54]. Similar methods have also been used to create porous GaN membranes, as discussed in the applications section.

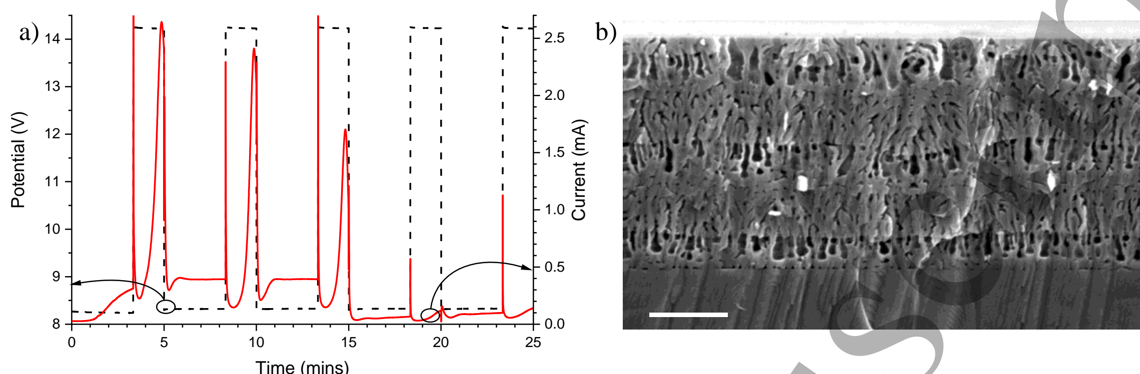

Figure 6: a) Potential (black, dashed) and current (red, solid) profiles for ECE of a single doped layer with periodic potential modulation and b) SEM image showing the resulting morphology.

Subsurface Pores

Creating porous layers below solid nitride material has been demonstrated in three ways: etching laterally from scribed trenches [55], using vertical pathways through dislocations in non-porous material [9] and by regrowing material on a structure that contains porous layers [56]. These methods have distinct pros and cons and together they offer a wide range of possible structures for different applications. Patterning trenches for the electrolyte to access subsurface doped layers and etch them laterally has been demonstrated by many groups [57–59]. This is done by growing a nitride structure containing one or more highly doped layers to be made porous. Access trenches are then scribed into the structure to the required depth and these expose the doped layers to the electrolyte, such that etching can proceed from them laterally. Electrical contact is made to the sample in order to create an electric field to the doped layers and create pores. An example of this is illustrated in Figure 7, where a porous layer (indicated as NP, for "nanoporous") has been created under an LED structure [60]. The pores are formed after the material growth, but before the device processing. In this case, trenches were formed by laser scribing (LS), but ICP-RIE can also be used [58]. Figure 7a shows an overview of a single LED chip with n and p pads and the LS lines between devices. Figure 7c-e show the strong pore alignment achieved in the NP layer, growing perpendicular to the LS lines. Creating straight pores with low branching can be achieved by tuning the etching parameters as discussed above.

Accepted Manuscript

1 2 3 4 5 6 7 8 9 10 11 12 13 14 15 16 17 18 19 20 21 22 23 24 25 26 27 28 29 30 31 32 33 34 35 36 37 38 39 40 41 42 43 44 45 46 47 48 49 50 51 52 53 54 55 56 57 58 59 60

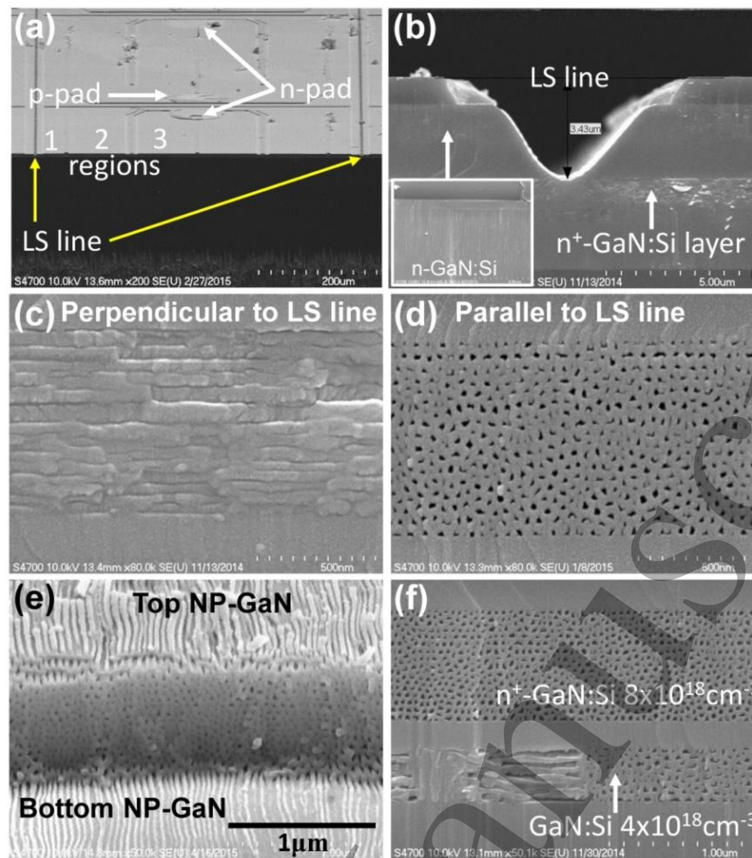

Figure 7: SEM images of a porous layer formed underneath an LED structure. (a) shows an oblique overview of the LED, (b), the cross-section at a laser scribed (LS) line between 2 LED chips with an inset image of the undesired porosity in the n-LED layer, cross-section of the subsurface pores (c) perpendicular and (d) parallel to the LS lines, (e) oblique view of the porous layer where some of the structure has peeled away, showing nanopores aligned along the etching direction, and (f) cross-section showing pores in two differently doped layers near to the LS line. Reprinted with permission from [60], © The Optical Society.

A challenge of this method is preventing etching of other doped layers in the structure, in this case the n-GaN of the LED itself. The structure shown in Figure 7 contained three n-GaN, Si-doped layers prior to etching. The topmost layer is the n-contact of the LED, labelled "n-GaN:Si" in Figure 7b. The second layer is exposed by the LS trenches and is more highly doped, labelled "n^+-GaN:Si" in Figure 7b and with a nominal doping density of $8\times10^{18}cm^{-3}$. This the layer that is intended to be porosified. Below this is a third n-doped layer with a lower doping density of $4\times10^{18}cm^{-3}$, which was used to make electrical contact for the ECE process. Figure 7b shows the cross-section around the LS line, which indicates undesired porosity in the n doped layer of the LED and Figure 7f shows the same in the contact layer. The researchers found that the higher doping density for the NP layer resulted in a higher etch rate than for the other doped layers. As the electrical contact was made to the lower doped layer the increasing resistance of the NP layer as it becomes porous also acts to lower the potential seen by the n-LED layer. These factors resulted in the n-LED layer only becoming porous close to the LS lines, as seen in Figure 7b (inset). This does make it difficult to have highly doped non-porous layers on top of porous layers using this method. A SiO_2 layer was also deposited onto the top-surface prior to laser scribing, in order to prevent surface etching, which is very commonly used in this method. Other work has deposited a protective layer after the trenches are scribed in order to passivate the side walls and prevent unwanted pores forming [61]. Etching access trenches adds some complexity to the fabrication process, but with careful design to prevent unwanted etching it offers a flexible system for pore formation and has been demonstrated for single layers and multilayer structures, most notably in forming DBRs [55,62].

The second approach to forming subsurface pores is a remarkable method, by which multiple layers of buried n-doped material can be porosified across whole wafers with almost no measurable change to the surface or the NID layers separating them [9]. The big advantage of this approach is that it can be used to create multiple layers of subsurface porosity across whole wafers in a single processing step without any prior patterning. The process is very similar to the first method, described above, but instead of providing access trenches to the

Accepted Manuscript

1
2
3
4
5
6
7
8
9
10
11
12
13
14
15
16
17
18
19
20
21
22
23
24
25
26
27
28
29
30
31
32
33
34
35
36
37
38
39
40
41
42
43
44
45
46
47
48
49
50
51
52
53
54
55
56
57
58
59
60

subsurface layers the etching proceeds vertically from the top surface down into the structure through dislocation pathways. The non-intentionally doped surface and barrier layers are almost entirely left intact, while the doped layers become porous. Our recent work used plan-view high angle annular dark field imaging in the scanning transmission electron microscope (HAADF-STEM) imaging to understand this process using a porous GaN DBR [63]. Figure 8a shows an edge dislocation in the structure prior to ECE, showing a typical core structure consisting of a five-membered and a seven-membered ring, whereas after ECE Figure 8b shows a hollow core at the centre of an edge or mixed dislocation, identified by the Burgers circuit diagram. This demonstrates that dislocation cores in the NID layers are being etched by the ECE process in order to provide pathways for the etching of doped material at lower layers. The lower magnification HAADF-STEM image in Figure 8c shows the morphology in the porous layers. Fern-like pore structures are visible, which branch out radially from dislocation cores, one of which is ringed with a white circle. The pores spread out from the cores to form domains as highlighted by the yellow lines. Where the domains meet, a boundary of un-etched material is observed. The size of the domains depends on the proximity of other dislocation cores. Perhaps surprisingly, this method has also been shown to work in an alkaline electrolyte [64].

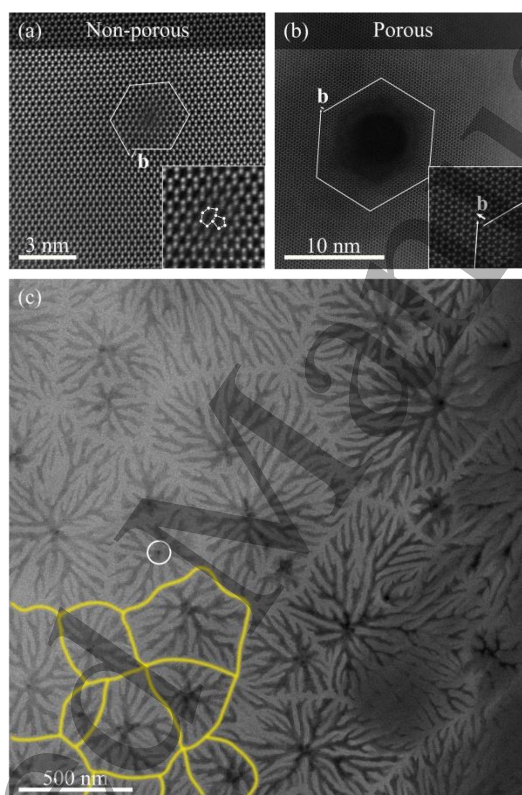

Figure 8: High resolution HAADF-STEM image of a dislocation seen along the <0001> zone axis (i.e. seen end-on). (a) a non-porous GaN DBR sample, and (b) a porous GaN DBR sample. (c) Lower magnification HAADF-STEM image of a porous layer in the porosified sample. Contrast is thickness-related (i.e. dark means pore). The white circle highlights a dislocation core and the yellow lines highlight the porous cells formed around individual dislocations. Reprinted from [63].

One limitation to this vertical etching method is the challenge of defining which regions become porous horizontally across the wafer. This is straight forward to achieve in the lateral method through the design of the patterned trenches. Devising a method for horizontal patterning of the vertical etch method could provide a powerful system for forming defined pads of subsurface porosity where required, for applications such as providing thermal insulation for sensors [65]. We have explored this approach by using simple lithography techniques to block the electrolyte from accessing dislocation pathways in certain regions. The patterning material must be insoluble and impermeable to the electrolyte in order to protect the underlying surface effectively. We have found that commercial, Microposit photoresist can be used to achieve this, which allows standard photolithography techniques to be used. 200 μm wide stripes were formed using photoresist on the surface of a sample with a 1 μm thick n-doped GaN layer topped by a 200 nm thick NID GaN cap and the ECE method described elsewhere was applied [9].

Accepted Manuscript

1
2
3
4
5
6
7
8
9
10
11
12
13
14
15
16
17
18
19
20
21
22
23
24
25
26
27
28
29
30
31
32
33
34
35
36
37
38
39
40
41
42
43
44
45
46
47
48
49
50
51
52
53
54
55
56
57
58
59
60

Figure 9a shows an optical image of this sample, showing porous material in the un-protected regions and nonporous material under the photoresist, which are indicated by the blue shading. There is some leakage of porosity underneath the photoresist, which is highlighted at one edge by the yellow line in Figure 9a. The cross-sectional SEM image in Figure 9b shows the porous region leaking under the protective photoresist layer. The challenge of achieving a well-defined line between the porous and non-porous regions is that the process uses randomly distributed dislocation pathways to access the doped layer. Where uncovered dislocations lie close to the photoresist they can create porosity for a large distance underneath it, but in other regions there are no dislocations near the photoresist and the leakage is less. This can be seen by the variation in distance between the photoresist edge and the yellow line in Figure 9a. This sample has a thicker NID GaN capping layer than the previous work with DBRs. This leads to larger circular domains of porous material, as measured optically, than was seen for DBRs and suggests that the density of nanopipe formation is lower. A straighter line could therefore be produced more easily for material with thinner capping layers, as the variation in distance from the nearest uncovered dislocation will be less. This will still produce leakage underneath the protective layer, which would need to be factored in when defining the pattern and will lower the minimum achievable line thickness. For PECE, lateral patterning can also be achieved using a metal layer that blocks the light [66].

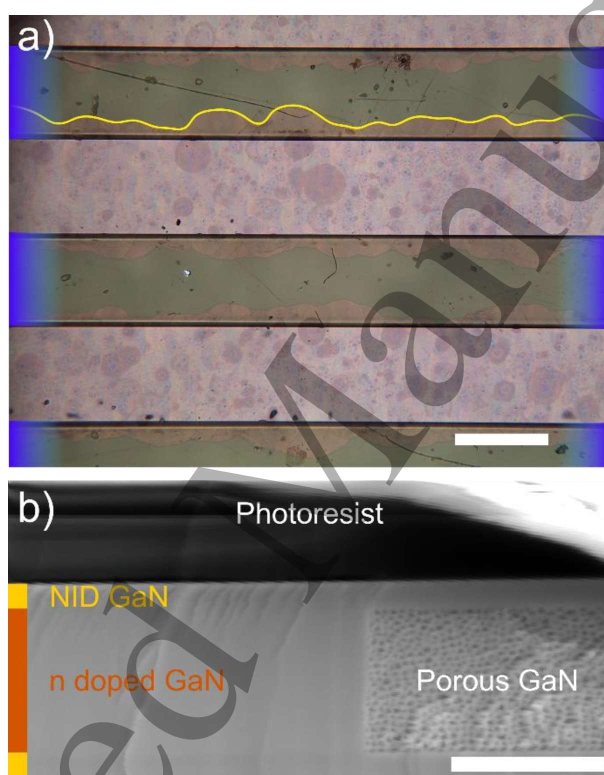

Figure 9: a) Optical image showing surface patterning of a 1 μm thick subsurface porous layer. The blue shading indicates either end of each photoresist stripe, the yellow line shows the line of the porous material that has “leaked” underneath the photoresist at one boundary. The scale bar is 200 μm. b) Cross-sectional SEM image of the same sample, showing porosity leaking slightly under the protective photoresist. Scale bar is 1 μm.

The two methods for forming subsurface pores outlined above (lateral etching through access trenches and vertical etching through dislocations) are both limited by the difficulty of producing a structure with a highly doped layer above a porous layer. A third approach to forming subsurface pores overcomes this by forming the desired porous layers and then returning the sample to the reactor to grow more material on top. This eliminates the risk of unintended pores being formed in the higher layer, meaning the regrown layers can be highly doped. This method has been demonstrated to improve LED performance for both single porous layers on silicon substrates [67], as well as porous DBRs produced using vertical etch pathways on sapphire [10]. The pore morphology can be altered during regrowth, depending on the growth temperature used. Yang et al. found that annealing a porous GaN DBR at 950°C enhanced the specular reflectivity significantly, whereas annealing at 1100°C lowered it severely due to the resulting change in pore morphology [68]. These porous structures improved light-extraction efficiency significantly, and other applications of overgrowth on porous structures are discussed in the applications section.

Accepted Manuscript

1 2 3 4 5 6 7 8 9 10 11 12 13 14 15 16 17 18 19 20 21 22 23 24 25 26 27 28 29 30 31 32 33 34 35 36 37 38 39 40 41 42 43 44 45 46 47 48 49 50 51 52 53 54 55 56 57 58 59 60

Porous Nitrides other than GaN

So far, almost all of the discussion has been around forming porous GaN, as this has been where the bulk of research efforts on porous nitrides have been focussed, but a key characteristic of nitride devices is the use of other alloys in the family of nitride semiconductors. Initial work seems to suggest that forming pores in these materials follows much the same path as for porous GaN with few material specific deviations, therefore the description of the depletion model presented for the formation of pores in GaN above provides a useful starting point for the development of pores in other nitride alloys. Electropolishing in order to selectively remove InGaN layers to form an undercut has been demonstrated in order to create microdisk lasers [69]. This uses a difference in bandgap to select which layers to etch. All the work we could find in the literature to form bulk porous material from In containing nitrides through anodization came from one group and uses both HF and KOH based electrolytes [70,71] and explores the influence of the light source, finding that anodization without illumination produced etching only at grain boundaries and other inhomogeneities, whereas incident light allows the formation of surface pores [72]. This results in a limited pore depth, corresponding to the absorption length of the incident light. It has been reported that increasing etch time increases the porosity of these InGaN layers [71] and similar work has been done for InAlGaN, showing an increase in surface pore density with increasing etch time under PECE in KOH [73]. Comparing to results with GaN, this may suggest that this etching is occurring in a low-potential, pre-breakdown regime [31]. Although ECE of InGaN in KOH failed to form pores without illumination, it could be that a higher applied potential or N_D would allow the formation of pores, but this is not explored [72]. Indeed, ECE of InGaN in a HF based electrolyte does show surface pores, but as these samples were etched under constant current the applied potential is not reported, and N_D is not reported for either so it is difficult to make a comparison [70]. We have found that subsurface Si-doped InGaN layers can be porosified in much the same way as GaN layers. As an example, Figure 10 shows a cross-sectional SEM image of a porosified $In_xGa_{1-x}N$ layer with x=12% on GaN on sapphire with a 100 nm GaN cap. The InGaN was porosified at 7 V in oxalic acid. Pores can also be seen at the sapphire GaN interface, which arises when an unintentionally doped layer is present at this interface, as has been observed previously [74].

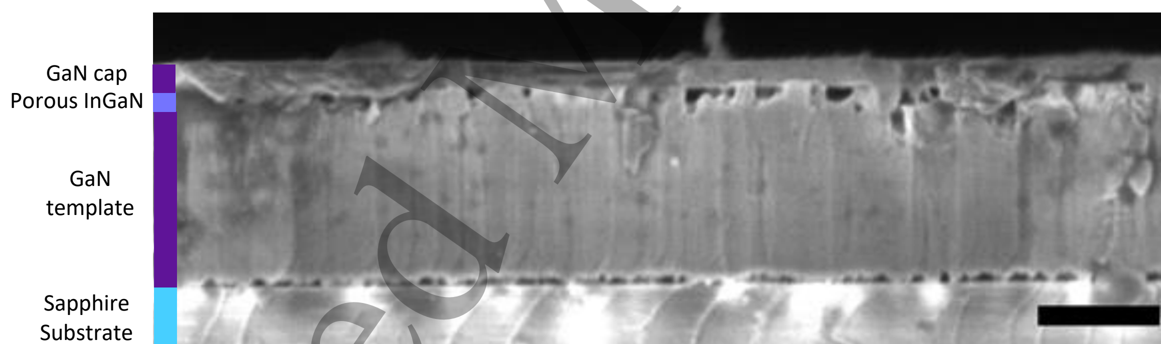

Figure 10: Cross-sectional SEM image of a porous InGaN layer. Scale bar is 500 nm.

For alloys containing aluminium, we have demonstrated periodic structures of $Al_{0.6}Ga_{0.4}N$ using ECE in oxalic acid, following the same ECE methods developed for porous GaN, although AlGaN's lower conductivity necessitates a higher applied potential for similar morphology [75]. Similarly, surface porous $Al_{0.55}Ga_{0.45}N$ has been created using ECE in KOH [76]. Lateral etching of subsurface porous layers shows that ECE with KOH has much less doping selectivity than using HNO_3. KOH formed triangular pores that were not well confined to the doped layers by exposing $\{10\bar{1}\bar{1}\}$ surfaces, whereas etching with acidic electrolytes forms oval pores, which are well confined to the doped layers [77]. Porous AlGaN layers have also been demonstrated through lateral etching in a subsurface doped layer from an etched hole when the applied potential was too low to completely remove the doped layer and create a membrane [78]. In this work, they show the same trend of increasing pore size with applied potential, and also find that higher AlN content requires a higher potential to remove the doped layer. This is attributed to a reduction of the electron affinity with increasing AlN content, which increases the depletion width.

Photoelectrochemical etching of AlGaN structures is more challenging with increasing AlN content, as the absorption efficiency reduces. PECE electropolishing of AlGaN has been reported for AlN content up to 20% [79]. This method shows a slower etch rate than for GaN, due to lower light absorption [80]. We could find little

Accepted Manuscript

1
2
3
4
5
6
7
8
9
10
11
12
13
14
15
16
17
18
19
20
21
22
23
24
25
26
27
28
29
30
31
32
33
34
35
36
37
38
39
40
41
42
43
44
45
46
47
48
49
50
51
52
53
54
55
56
57
58
59
60

reported work to produce porous AlGaN via PECE, although voids have been created in low AlN content AlGaN using a heterostructure [81] and surface pores have been reported, although it is unclear as to whether these pores penetrate the surface with significant depth, or are merely a surface roughening effect [82]. The use of PECE adds another dimension when forming pores in nitride heterostructures, as control of the etching process can be achieved through bandgap specific absorption. For example, InGaN has a lower bandgap than the other nitride semiconductors, meaning that by controlling the photon energy of the incident light InGaN can be etched while leaving other material intact. In this way it has been used as a sacrificial layer [83–85], as well as using AlGaN (a higher bandgap material) as an etch stop when etching GaN [66]. Seeing as high doping selectivity has been widely demonstrated for porosification and doping does not change the lattice constant, this approach has not been widely demonstrated to form porous nitrides. Bandgap selectivity has been used with PECE to tune the size of InGaN quantum dots [51]. An InGaN layer etches under PECE to form dots. The etching terminates when the dots reach a critical size, which is determined by the absorption wavelength reducing to below the wavelength of the incident light. As well as InGaN and AlGaN, PECE of the quaternary InAlGaN structure has also been used to produce pores, using a HF electrolyte [86].

In this section, we have shown that a large range of porous nitrides can be produced through anodization and that the resulting morphology depends strongly on potential, doping density, how illumination is used and can also be influenced by the choice and concentration of electrolyte. There are certainly multiple ways to achieve similar morphologies and as yet there is no definitive comparison across these four parameters.

Applications

We have seen how porous nitrides can be created with various morphologies in a wide range of structures. We'll now discuss the applications for which porous nitrides are being developed. The wide range of applications being considered is testament to the versatility of porous nitride structures. These applications include the improvement of LED and laser performance, chemical and thermal sensors, as well as the use of porosity to relax strain and reduce dislocation density.

Optical Devices

DBRs are key components for forming optical cavities and creating vertical cavity surface emitting lasers (VCSELs), as well as increasing the extraction efficiency of LEDs. They are periodic superlattices of two materials with differing refractive index that are designed to have high reflectivity for a given target wavelength. This is done by choosing the thickness of each layer to be a quarter of the target wavelength in that material, such that constructive interference leads to a strong reflection peak. Unlike the GaAs material system, epitaxial DBRs are very challenging to fabricate in the nitrides, due to the constraints of strain and the limited range of refractive index [87]. AlInN with InN content around 18% is lattice-matched to *c*-plane GaN and a superlattice of the two can be grown without building up strain [88], but the refractive index contrast between the two is small, meaning that many repeats and therefore a long growth time are required to obtain high reflectivity [89]. There is no available pair of materials which allows lattice matching along all directions on a non-polar nitride surface. Porous DBRs have the potential to overcome these problems, as they can be grown as a single alloy with periodic doping variation and therefore no difficulties with strain, but when porosified they have much greater refractive index contrast between the layers, which results in far fewer lattice pairs being necessary for high reflectivity and therefore shorter growth times. A porous DBR has been demonstrated in this way with reflectivity >99.5% and a much wider stop-band than epitaxial GaN DBRs with similar reflectivity [8]. These structures also show electrical conductivity after ECE, meaning they can be used for electrical injection [9]. Figure 11 shows the structure of the first electrically injected nitride VCSEL with a bottom porous DBR, made on m-plane GaN [90]. This exhibited record optical output power for an m-plane GaN VCSEL of 1.5 mW. The DBR was laterally etched via RIE etched trenches using ECE in oxalic acid. The polarization of the light output was linearly polarized in the a-direction, which suggests that optical scattering from the DBR was negligible. One concern with these structures is thermal conductivity. We have shown that this can be reduced by more than an order of magnitude by creating pores, which can be used for on-chip thermal insulation for high sensitivity thermal sensors [65]. For most optoelectronic devices this would pose a heat management problem, but recent analysis suggests that optimisation of pore morphology can allow for high electrical and thermal conductivity while still maintaining reasonable refractive index contrast when compared to the epitaxial and dielectric alternatives [91]. Porous GaN has also been used in edge emitting lasers to provide lateral optical confinement through a novel, tapered porous layer [92].

Accepted Manuscript

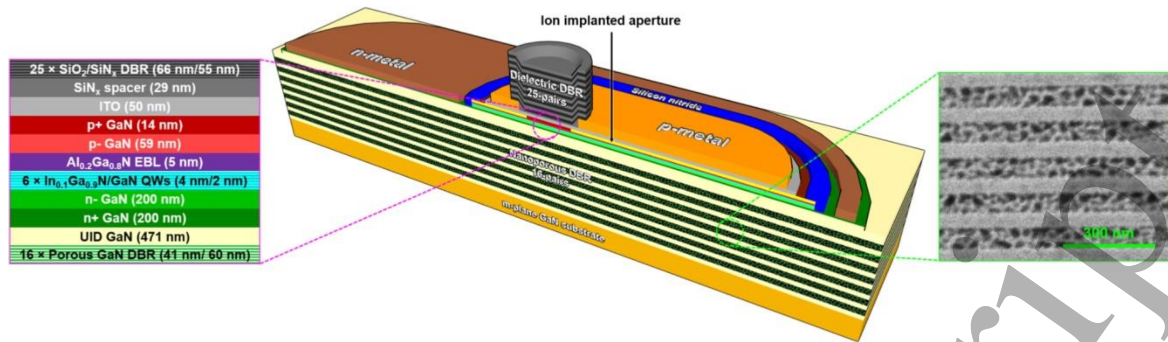

Figure 11: Cross-sectional schematic of an m-plane VCSEL with bottom porous DBR and (right) an SEM image of the DBR. Reprinted from [90], with permission of IOP publishing.

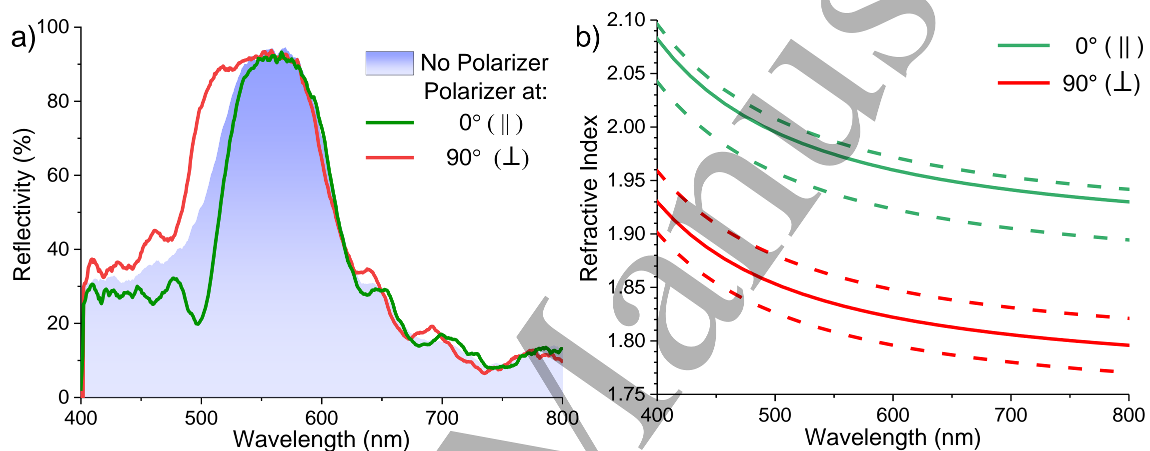

Figure 12: (a) Optical reflectivity spectra obtained from a laterally etched DBR with different polarization conditions. The blue shaded curve is collected with no polarizers, while the coloured, solid lines are taken with the analyser aligned ∥ and ⊥ to the pores. These data are referenced to give an absolute reflectivity value for each polarisation condition. (b) Shows the effective refractive index of the porous GaN layer obtained by fitting a transfer matrix model to the data in (a). The solid lines show the best estimate and the dashed lines give the spread of the uncertainty. Reprinted from [93].

Porous GaN has also been shown to exhibit birefringence if the pores are strongly aligned [60]. This offers a powerful tool for incorporating polarisation engineering into GaN optical devices. Our recent work has explored the mechanisms for this in detail by using advanced FIB-SEM imaging techniques to reconstruct the 3D morphology of porous GaN DBRs formed through both lateral and vertical channel etching. We then explored the relationship between the morphology and the observed birefringence by correlating it with finite element modelling [93]. Figure 12a shows measured reflectivity spectra of a porous GaN DBR that was etched laterally from scribed trenches, leading to highly aligned pores. The Figure shows the reflectivity of the structure with different incident polarisation. When the incident light is polarised parallel to the pore direction (0°, ∥), the stopband width is much narrower than when the light is polarised perpendicular to the pores (90°, ⊥) and the result for non-polarised light lies in between the two. This indicates that the effective refractive index of the porous GaN layers is a function of polarisation. By fitting the reflectivity stopbands with a transfer matrix model, which assumes a constant refractive index for each porous layer, the effective refractive index can be measured, as plotted in Figure 12b. This shows a strong birefringence of the porous GaN layers of Δn=0.14 ±0.05 at 500 nm, with a lower refractive index parallel to the pores than perpendicular to them. This puts it among the most strongly birefringent natural materials, such as calcite (with $\Delta n \approx$ -0.17 across the visible range [94]). The modelling shown in this work suggest that the degree of birefringence depends strongly on the size of the gaps between pores, suggesting that higher birefringence is possible from optimised porous GaN structures.

Accepted Manuscript

1
2
3
4
5
6
7
8
9
10
11
12
13
14
15
16
17
18
19
20
21
22
23
24
25
26
27
28
29
30
31
32
33
34
35
36
37
38
39
40
41
42
43
44
45
46
47
48
49
50
51
52
53
54
55
56
57
58
59
60

Porous DBRs have also been demonstrated in UV photodetectors for light recycling [95]. This uses a GaN active layer with an AlGaN DBR below it, such that absorption losses are minimised in the DBR. This increases both the responsivity and sensitivity at the tuned wavelength. Porosity in the active region of nitride photodetectors has also been demonstrated [59,70,96–98] with porous GaN showing improved performance compared to bulk GaN devices and high detectivity in the UV [59]. This is attributed to high internal gain from charge trapping of carriers at the semiconductor metal interface. The porous structure will also create light trapping and reduce reflection.

Piezoelectric Devices

Nitride semiconductors have large piezoelectric constants, making them of particular interest for piezoelectric sensors and nanogenerators [99,100]. In order to benefit from this, the material must be compliant, but due to GaN's high stiffness this requires the use of structures like membranes or nanowires. A further barrier for using nitrides in these devices is the high conductivity that reduces the piezoelectric field by carrier screening, but in structures such as nanowires the large surface area can suppress this through Fermi-level pinning. This has been demonstrated using ECE to undercut GaN structures to create membranes for piezoelectric nanogenerators (PNGs) [101]. Porosity offers a way of reducing stiffness and suppressing carrier screening in a similar way to nanowire arrays, but through a cheap and versatile fabrication approach. Porous GaN PNGs have been demonstrated with both laterally and vertically etched pores [102,103]. Figure 13 shows the output of a laterally porous PNG with three different porosities. The highly porous device shows significantly larger output power than the less porous devices due to a higher degree of Fermi-level pinning at the surfaces of the pores, which acts to suppress carrier screening. The piezoelectric size effect also enhances the piezoelectric constants of surface layers, as compared to the bulk values [102].

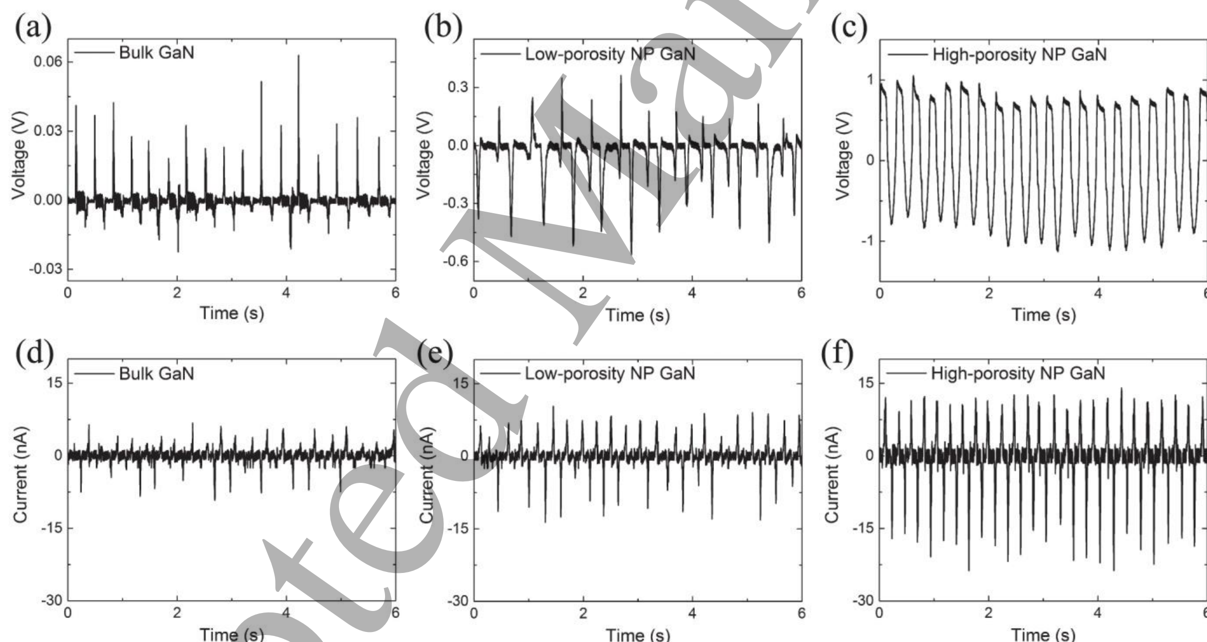

Figure 13: Output voltage and current under periodic pressing and releasing measured from (a), (d) bulk, (b), (e) low-porosity, and (c), (f) high-porosity porous (labelled NP, for “nanoporous”) GaN piezoelectric nanogenerators with lateral porosity. The porosity of the bulk, low- and high-porosity GaN is 0%, 18%, and 38%, respectively. Reprinted from [102], with permission of IOP publishing.

Chemical Devices

The use of GaN in chemical sensing is well-documented due to its high temperature tolerance and chemical inertness, which make it particularly suited to sensing in extreme environments. Nanostructuring increases the surface area of the device, which can increase sensitivity, but the advantages of nanostructuring through nanowire growth are hampered by poor reproducability [104]. Porous nitrides offer a straightforward fabrication method for nanostructuring material, which may be able to overcome the fabrication challenges seen in nanowires. Sensing of myriad different species in liquid and gas has been demonstrated using porous nitrides. Liquid sensors use a porous nitride electrode in an electrochemical cell. Many of these use a composite material

Accepted Manuscript

1
2
3
4
5
6
7
8
9
10
11
12
13
14
15
16
17
18
19
20
21
22
23
24
25
26
27
28
29
30
31
32
33
34
35
36
37
38
39
40
41
42
43
44
45
46
47
48
49
50
51
52
53
54
55
56
57
58
59
60

with metal nanoparticles deposited into the porous matrix [4,105,106], while the detection of Ag(I) ions has been demonstrated using a porous GaN electrode with no further deposition process [107]. Simple hydrogen gas sensors have also been demonstrated using Pt contacts on an InAlGaN layer [86]. Porosifying the InAlGaN layer via PECE lead to better sensitivity, lower power consumption and faster response time, compared to the non-porous InAlGaN device. More recent work has passivated the porous surface by sulfur treatment and functionalised the surface with Pt nanoparticles [3]. This device showed high sensitivity to H_2 down to 30 ppm. Work towards porous GaN sensors is in its infancy, and whilst there have been demonstrations of advantages over bulk GaN devices they must show long-term stability and high reproducability if they are to be of real commercial interest.

Catalysis, in particular for water-splitting applications, is a huge area of research pursuing a source of hydrogen fuel with no direct CO_2 emissions [108]. The nitrides have ceramic like stability, while offering high electrical conductivity and a wide bandgap, as well as offering band edge potentials that allow hydrogen generation at zero bias, making them of keen interest as electrodes in such systems [5,109]. Porosification creates a much higher surface area and enhanced light absorption due to scattering, which can dramatically improve catalysis effiency [110], as well as increasing the electrode stability [111]. Porous GaN electrodes have also been demonstrated as photocatalysts for the breakdown of organic molecules, showing superior performance compared to both bulk nitride and to porous Si electrodes [5]. Porosity has been combined with conventional lithography techniques to create composite porosity, whereby structures combine pores at two different scales, which increases absorption even further and thereby increases catalytic photocurrent [112]. As we have seen, porosity can vary a lot between porous nitride samples and the pore morphology has a strong effect on the photon conversion efficiency [113]. While many promising early results have been produced, optimisation of the structure and demonstration of H_2 production over long lifetimes are yet to be demonstrated.

Composite Devices

Porous nitrides offer the possibility of producing composite materials through the infiltration of the pores with another species. Porous GaN offers a robust, conductive scaffold that can provide electrical transport to a wide variety of materials. We have already discussed examples of porous GaN composite devices, where porous GaN is infiltrated with metal nanoparticles for chemical sensing [3,4,105,106]. The choice of nanoparticle can functionalise the device to provide a chemical selective response. The particular strength of porous nitrides for these sensors is their chemical and mechanical robustness, making them suitable for harsh environments and offering long-term stability.

Beyond nanoparticles, we have demonstrated infiltration of porous GaN with lead-bromide perovskites, such that the GaN acts to encapsulate the material and dramatically increase its lifetime [7]. This offers a number of advantages. Firstly, as shown in the PL spectra of Figure 14, the encapsulation offered by the porous GaN matrix serves to protect the perovskite from decomposition in the atmosphere. After 10 days in ambient air, the PL signal is preserved when deposited on porous GaN, but drops significantly when deposited on glass or planar GaN. Moreover, the porous GaN sample still showed a bright PL signal after almost a year. The second advantage is in terms of light extraction, as the porous structure will help to scatter light out of the device [114]. This may be one reason why the as-deposited PL signal is stronger for the porous GaN sample in Figure 14. This suggests that this method could be relevant to colour-conversion layers on nitride LEDs, which simultaneously increase light extraction efficiency. Beyond this a porous nitride layer could provide electrical injection into solution processed semiconductor devices. This opens up opportunities for hybrid organic/inorganic optical devices, where the advantages of one can compensate the disadvantages of the other.

Accepted Manuscript

1
2
3
4
5
6
7
8
9
10
11
12
13
14
15
16
17
18
19
20
21
22
23
24
25
26
27
28
29
30
31
32
33
34
35
36
37
38
39
40
41
42
43
44
45
46
47
48
49
50
51
52
53
54
55
56
57
58
59
60

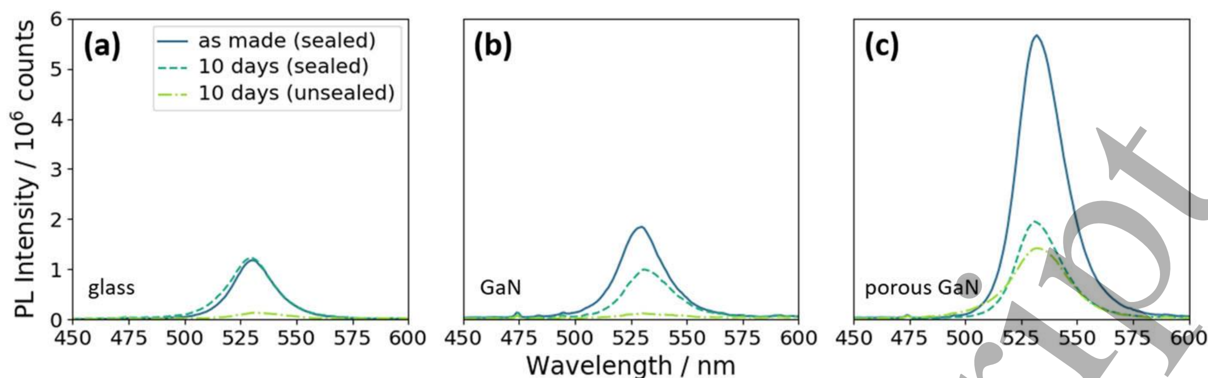

Figure 14: PL spectra for MAPbBr3 perovskite deposited on (a) glass, (b) non-porous GaN, and (c) porous GaN, indicating the decrease in PL intensity after 10 days in ambient atmosphere with and without epoxy-glass sealing. Reprinted from [7], published under a creative commons license.

Improving Material Quality

Reducing dislocation density is an important area of research in the nitrides. Using porous layers as growth templates has been shown to relax strain, which reduces the density of dislocations formed as well as blocking threading dislocations from propagating. Strain relaxation in GaN grown on porous GaN was reported as early as 1999 of a 3 µm thick GaN layer grown by HVPE and producing low roughness and high crystalline quality [115]. Many sources demonstrate strain relaxation in nitride films grown on porous nitride surface layers compared to bulk templates, indicated by both Raman [12,50,67,115] and XRD [34,56] data. A study of PECE GaN grown on sapphire found that crystalline quality and relaxation of compressive stress increase with etching current, but there is yet to be a detailed study to find the optimal conditions for the strain relief of regrown layers.

To demonstrate the improvement in material quality from porous templates, LEDs have been regrown on porous structures. These see enhancement in the electroluminescence output due to decreased leakage, greater extraction efficiency due to light scattering at the porous layer, increased internal quantum efficiency due to higher material quality and increased carrier confinement due to reduced quantum confined stark effect (QCSE) from lower strain fields [34,50,67,116]. Reduced strain fields have also been indicated as the cause of a blue-shift in the band-edge luminescence peak for GaN layers grown on porous GaN [34]. In our own work we have regrown LEDs on porous DBR templates and although there was significant enhancement from other effects, we did not find evidence of strain relaxation from XRD, or blueshift in the luminescence due to reduced QCSE [10]. This suggests that porosity must be on the template surface in order to provide strain relief for the regrown layer. As well as strain relief, reduction of the FWHM of XRD rocking curves has been used to suggest that films grown on porous templates have lower dislocation density [49,67] and this has also been shown in AlGaN grown on porous and non-porous GaN templates shown by AFM measurements after acid treatment to expose dislocations [56]. It has been suggested that part of this comes from the annihilation of threading defects at voids forming in the porous layer during regrowth [117]. However, XRD data from other, similar work showed a negligible reduction in dislocation density [34]. This indicates that there is a need for optimisation of the process for maximum dislocation reduction, as the difference in results seems to arise from the very different pore morphologies that were regrown on.

Mechanical Lift-off

As well as using porous nitrides in devices, there has been promising development of using ECE and PECE as processing steps for lifting off nitride devices so that they can be transferred to alternative substrates. This is of interest as a way to overcome some of the limitations of sapphire substrates, such as thermal conductivity [118], as well as making growth on GaN substrates more economical, by allowing substrate reuse [119]. Lift-off on UV transparent substrates, such as sapphire can be achieved via laser lift-off, but chemical methods are required for lift-off from GaN substrates. Porous GaN membranes have been created through both ECE [120] and PECE [13]. This process etches from the surface of the sample to create pores through the structure and can be released by pushing the etching into the electropolishing regime by either increasing the etching potential (as in Procedure A) or the doping density, N_D (as in Procedure B) as shown in Figure 15. The limitation of this method is that the membranes must be porous, although membranes of porous GaN DBRs have been created

Accepted Manuscript

1
2
3
4
5
6
7
8
9
10
11
12
13
14
15
16
17
18
19
20
21
22
23
24
25
26
27
28
29
30
31
32
33
34
35
36
37
38
39
40
41
42
43
44
45
46
47
48
49
50
51
52
53
54
55
56
57
58
59
60

from structures with modulated doping that leads to high porosity layers and almost non-porous layers using the wafer-scale method via dislocation pathways [121].

These processes produce flexible single-crystal GaN membranes showing strain relaxation. In order to produce non-porous membranes, an alternative lift-off approach uses access trenches to create undercutting. This has been demonstrated using ECE to lift-off 90 nm thick nonporous membranes, which are depleted, due to the joining of the two surface depletion regions, allowing the creation of normally off transistors [14]. These novel demonstrations show the flexibility of electrochemical etching techniques in the nitrides. In terms of device lift-off, a PECE approach has been developed to allow the batch processing of flip-chip LEDs to allow GaN substrate reuse. Here, a SiN_x layer was used to protect the devices from the PECE process, while unprotected sacrificial layers were undercut, allowing the release of the devices and transfer to an alternative substrate [122].

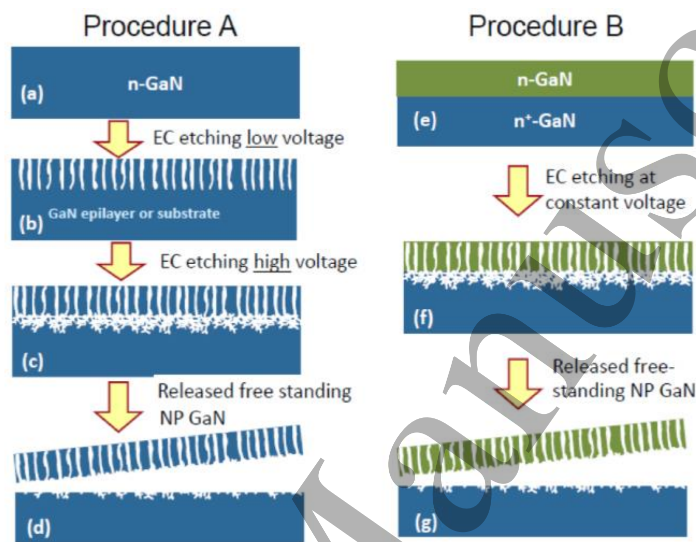

Figure 15: (a)–(g) Schematic drawings of two procedures to produce free-standing porous GaN membranes using ECE. Procedure A uses an increase in the applied potential to release the membrane, while Procedure B uses an increase in the material's doping density (N_D). Reprinted from [120], with permission of IOP publishing.

Summary

Porous nitrides are a fast developing research area for the nitrides that open up new application spaces for nitride semiconductors by allowing material parameters to be changed in a whole new way. The refractive index, thermal conductivity, birefringence and surface area can all be engineered with porosity in a highly controllable way through ECE and PECE. Control of these methods relies principally on controlling the local electric field strength between the material and the electrolyte. To facilitate etching, doped layers must be in contact with the electrolyte, either at an exposed surface or, interestingly, via nanoscale channels such as those formed at dislocation cores. A key challenge of incorporating porous material into practical devices is to find ways of preventing unwanted etching of other doped regions in the device. The three approaches of etching directly, etching via trenches and regrowing material on porous structures offer a flexible choice for achieving practically any required structure. Porous DBRs have an exciting application in forming cavities for VCSELs, which has been an ongoing challenge for the nitrides. By using porosity in AlN and AlGaN, this method can be extended into the UV, where efficient light emission is particularly challenging. More generally, the potential of porous layers as strain-relief to improve material quality has the potential to benefit all aspects of nitride semiconductors. Beyond these areas, considerable effort is being pursued in sensing applications, where the high surface area transforms the sensitivity of GaN. This is also an area that has seen porosity used as a method for creating hybrid materials, which offers a broad playground for creating novel material properties.

Acknowledgements

The authors gratefully acknowledge funding from the EPSRC under grant numbers: EP/M010589/1, EP/L015455/1, and EP/R511675/1.

Accepted Manuscript

1
2
3
4
5
6
7
8
9
10
11
12
13
14
15
16
17
18
19
20
21
22
23
24
25
26
27
28
29
30
31
32
33
34
35
36
37
38
39
40
41
42
43
44
45
46
47
48
49
50
51
52
53
54
55
56
57
58
59
60

References

[1] Humphreys C J 2008 Solid-State Lighting *MRS Bulletin* **33** 459–470

[2] Amano H, Baines Y, Beam E, Borga M, Bouchet T, Chalker P R, Charles M, Chen K J, Chowdhury N, Chu R, Santi C D, Souza M M D, Decoutere S, Cioccio L D, Eckardt B, Egawa T, Fay P, Freedsman J J, Guido L, Häberlen O, Haynes G, Heckel T, Hemakumara D, Houston P, Hu J, Hua M, Huang Q, Huang A, Jiang S, Kawai H, Kinzer D, Kuball M, Kumar A, Lee K B, Li X, Marcon D, März M, McCarthy R, Meneghesso G, Meneghini M, Morvan E, Nakajima A, Narayanan E M S, Oliver S, Palacios T, Piedra D, Plissonnier M, Reddy R, Sun M, Thayne I, Torres A, Trivellin N, Unni V, Uren M J, Hove M V, Wallis D J, Wang J, Xie J, Yagi S, Yang S, Youtsey C, Yu R, Zanoni E, Zeltner S and Zhang Y 2018 The 2018 GaN power electronics roadmap *J. Phys. D: Appl. Phys.* **51** 163001

[3] Shafa M, Priante D, ElAfandy R T, Hedhili M N, Mahmoud S T, Ng T K, Ooi B S and Najar A 2019 Twofold Porosity and Surface Functionalization Effect on Pt–Porous GaN for High-Performance H2-Gas Sensors at Room Temperature *ACS Omega* **4** 1678–84

[4] Xi R, Zhang S-H, Zhang L, Wang C, Wang L-J, Yan J-H and Pan G-B 2019 Electrodeposition of Pd-Pt Nanocomposites on Porous GaN for Electrochemical Nitrite Sensing *Sensors* **19** 606

[5] Cao D, Xiao H, Xu H, Cui J, Gao Q and Pei H 2015 Enhancing the photocatalytic activity of GaN by electrochemical etching *Materials Research Bulletin* **70** 881–6

[6] Zhang M-R, Chen X-Q and Pan G-B 2016 The Fabrication and Photocatalysis of Gold Nanoparticles/Porous GaN Composite *ChemistrySelect* **1** 3159–62

[7] Lim K T P, Deakin C, Ding B, Bai X, Griffin P, Zhu T, Oliver R A and Credgington D 2019 Encapsulation of methylammonium lead bromide perovskite in nanoporous GaN *APL Materials* **7** 021107

[8] Zhang C, Park S H, Chen D, Lin D-W, Xiong W, Kuo H-C, Lin C-F, Cao H and Han J 2015 Mesoporous GaN for Photonic Engineering—Highly Reflective GaN Mirrors as an Example *ACS Photonics* **2** 980–6

[9] Zhu T, Liu Y, Ding T, Fu W Y, Jarman J, Ren C X, Kumar R V and Oliver R A 2017 Wafer-scale Fabrication of Non-Polar Mesoporous GaN Distributed Bragg Reflectors via Electrochemical Porosification *Scientific Reports* **7** 45344

[10] Jarman J C, Zhu T, Griffin P H and Oliver R A 2019 Light-output enhancement of InGaN light emitting diodes regrown on nanoporous distributed Bragg reflector substrates *Jpn. J. Appl. Phys.* **58** SCCC14

[11] Huo Q, Shao Y, Wu Y, Zhang B, Hu H and Hao X 2018 High quality self-separated GaN crystal grown on a novel nanoporous template by HVPE *Scientific Reports* **8** 3166

Accepted Manuscript

[12] Hartono H, Soh C B, Chua S J and Fitzgerald E A 2007 High Quality GaN Grown from a Nanoporous GaN Template *J. Electrochem. Soc.* **154** H1004–7

[13] Xiao H, Cui J, Cao D, Gao Q, Liu J and Ma J 2015 Self-standing nanoporous GaN membranes fabricated by UV-assisted electrochemical anodization *Materials Letters* **145** 304–7

[14] Xiong K, Park S H, Song J, Yuan G, Chen D, Leung B and Han J 2014 Single Crystal Gallium Nitride Nanomembrane Photoconductor and Field Effect Transistor *Adv. Funct. Mater.* **24** 6503–8

[15] Zhuang D and Edgar J H 2005 Wet etching of GaN, AlN, and SiC: a review *Materials Science and Engineering: R: Reports* **48** 1–46

[16] Pearton S J, Vartuli C B, Shul R J and Zolper J C 1995 Dry etching and implantation characteristics of III-N alloys *Materials Science and Engineering: B* **31** 309–17

[17] Kao C-C, Huang H W, Tsai J Y, Yu C C, Lin C F, Kuo H C and Wang S C 2004 Study of dry etching for GaN and InGaN-based laser structure using inductively coupled plasma reactive ion etching *Materials Science and Engineering: B* **107** 283–8

[18] Mileham J R, Pearton S J, Abernathy C R, MacKenzie J D, Shul R J and Kilcoyne S P 1996 Patterning of AlN, InN, and GaN in KOH-based solutions *Journal of Vacuum Science & Technology A* **14** 836–9

[19] Uhlir A 1956 Electrolytic Shaping of Germanium and Silicon *Bell System Technical Journal* **35** 333–47

[20] Canham L 1990 Silicon Quantum Wire Array Fabrication by Electrochemical and Chemical Dissolution of Wafers *Appl. Phys. Lett.* **57** 1046–8

[21] Wolkin M V, Jorne J, Fauchet P M, Allan G and Delerue C 1999 Electronic States and Luminescence in Porous Silicon Quantum Dots: The Role of Oxygen *Phys. Rev. Lett.* **82** 197–200

[22] Ram S K 2014 Electrical Transport in Porous Silicon *Handbook of Porous Silicon* ed L Canham (Springer International Publishing) pp 263–79

[23] Bisi O, Ossicini S and Pavesi L 2000 Porous silicon: a quantum sponge structure for silicon based optoelectronics *Surface Science Reports* **38** 1–126

[24] Zhang L, Wang S, Shao Y, Wu Y, Sun C, Huo Q, Zhang B, Hu H and Hao X 2017 One-step fabrication of porous GaN crystal membrane and its application in energy storage *Scientific Reports* **7** 1–9

[25] Mena J, Carvajal J J, Martínez O, Jiménez J, Zubialevich V Z, Parbrook P J, Diaz F and Aguiló M 2017 Optical and structural characterisation of epitaxial nanoporous GaN grown by CVD *Nanotechnology* **28** 375701

[26] Malvajerdi S S, Elahi A S and Habibi M 2017 A novel technique based on a plasma focus device for nano-porous gallium nitride formation on P-type silicon *Phys. Plasmas* **24** 043511

Accepted Manuscript

1
2
3
4
5
6
7
8
9
10
11
12
13
14
15
16
17
18
19
20
21
22
23
24
25
26
27
28
29
30
31
32
33
34
35
36
37
38
39
40
41
42
43
44
45
46
47
48
49
50
51
52
53
54
55
56
57
58
59
60

[27] Talapaneni S N, Park D-H, Choy J-H, Ramadass K, Elzatahry A, Al Balawi A S, Al-Enizi A M, Mori T and Vinu A 2016 Facile Synthesis of Crystalline Nanoporous GaN Templated by Nitrogen Enriched Mesoporous Carbon Nitride for Friedel-Crafts Reaction *ChemistrySelect* **1** 6062–8

[28] Minsky M S, White M and Hu E L 1996 Room-temperature photoenhanced wet etching of GaN *Appl. Phys. Lett.* **68** 1531–3

[29] Tseng W J, van Dorp D H, Lieten R R, Vereecken P M and Borghs G 2014 Anodic Etching of n-GaN Epilayer into Porous GaN and Its Photoelectrochemical Properties *J. Phys. Chem. C* **118** 29492–8

[30] Vajpeyi A P, Tripathy S, Chua S J and Fitzgerald E A 2005 Investigation of optical properties of nanoporous GaN films *Physica E* **28** 141–9

[31] Chen D, Xiao H and Han J 2012 Nanopores in GaN by electrochemical anodization in hydrofluoric acid: Formation and mechanism *Journal of Applied Physics* **112** 064303

[32] Hartono H, Soh C B, Chua S J and Fitzgerald E A 2007 Fabrication and characterization of nano-porous GaN template for strain relaxed GaN growth *phys. stat. sol. (b)* **244** 1793–6

[33] Lin C-F, zheng J, Yang Z, Dai J, Lin D, Chang C, Lai Z and Hong C S 2006 High-Efficiency Ingan-Based Light-Emitting Diodes with Nanoporous Gan:mg Structure *Applied Physics Letters* **88**

[34] Jang L-W, Jeon D-W, Polyakov A Y, Govorkov A V, Sokolov V N, Smirnov N B, Cho H-S, Yun J-H, Shcherbatchev K D, Baek J-H and Lee I-H 2014 Electrical and structural properties of GaN films and GaN/InGaN light-emitting diodes grown on porous GaN templates fabricated by combined electrochemical and photoelectrochemical etching *Journal of Alloys and Compounds* **589** 507–12

[35] Zhang C, Yuan G, Bruch A, Xiong K, Tang H X and Han J 2018 Toward Quantitative Electrochemical Nanomachining of III-Nitrides *J. Electrochem. Soc.* **165** E513–20

[36] Nowak G, Xia X H, Kelly J J, Weyher J L and Porowski S 2001 Electrochemical etching of highly conductive GaN single crystals *Journal of Crystal Growth* **222** 735–40

[37] Föll H, Langa S, Carstensen J, Christophersen M and Tiginyanu I M 2003 Pores in III–V Semiconductors *Advanced Materials* **15** 183–98

[38] Carstensen J, Christophersen M and Föll H 2000 Pore formation mechanisms for the Si-HF system *Materials Science and Engineering: B* **69–70** 23–8

[39] Lin C-F, Chen K-T, Lin C-M and Yang C-C 2009 InGaN-Based Light-Emitting Diodes With Nanoporous Microhole Structures *IEEE Electron Device Lett.* **30** 1057–9

[40] Quah H J, Ahmed N M, Hassan Z and Lim W F 2016 Surface Alteration of Planar P-Type Gallium Nitride to Porous Structure Using 50 Hz Alternating Current-Assisted Photo-Electrochemical Etching Route *J. Electrochem. Soc.* **163** H642–51

Accepted Manuscript

1
2
3
4
5
6
7
8
9
10
11
12
13
14
15
16
17
18
19
20
21
22
23
24
25
26
27
28
29
30
31
32
33
34
35
36
37
38
39
40
41
42
43
44
45
46
47
48
49
50
51
52
53
54
55
56
57
58
59
60

[41] Lim W F, Hassan Z, Ahmed N M and Quah H J 2018 Porous Formation in p-Type Gallium Nitride Films via 50 Hz Operated Alternating Current-Assisted Photo-Electrochemical Etching in Methanol-Sulfuric Acid Solution *J. Electrochem. Soc.* **165** H620–8

[42] Morrison S R 1980 *Electrochemistry at semiconductor and oxidized metal electrodes* (New York: Plenum Press)

[43] Schwab M J, Chen D, Han J and Pfefferle L D 2013 Aligned Mesopore Arrays in GaN by Anodic Etching and Photoelectrochemical Surface Etching *J. Phys. Chem. C* **117** 16890–5

[44] Solymar L, Walsh D and Syms R R A 2014 *Electrical Properties of Materials* (Oxford, New York: Oxford University Press)

[45] Weyher J L, Brown P D, Rouvière J L, Wosinski T, Zauner A R A and Grzegory I 2000 Recent advances in defect-selective etching of GaN *Journal of Crystal Growth* **210** 151–6

[46] Mishkat-Ul-Masabih S, Luk T S, Rishinaramangalam A, Monavarian M, Nami M and Feezell D 2018 Nanoporous distributed Bragg reflectors on free-standing nonpolar m-plane GaN *Appl. Phys. Lett.* **112** 041109

[47] Kumazaki Y, Matsumoto S and Sato T 2017 Precise Structural Control of GaN Porous Nanostructures Utilizing Anisotropic Electrochemical and Chemical Etching for the Optical and Photoelectrochemical Applications *J. Electrochem. Soc.* **164** H477–83

[48] Park J, Song K M, Jeon S-R, Baek J H and Ryu S-W 2009 Doping selective lateral electrochemical etching of GaN for chemical lift-off *Applied Physics Letters* **94** 221907

[49] Radzali R, Zainal N, Yam F K and Hassan Z 2014 Characteristics of porous GaN prepared by KOH photoelectrochemical etching *Mater. Res. Innov.* **18** 412–6

[50] Soh C B, Tay C B, Tan R J N, Vajpeyi A P, Seetoh I P, Ansah-Antwi K K and Chua S J 2013 Nanopore morphology in porous GaN template and its effect on the LEDs emission *J. Phys. D: Appl. Phys.* **46** 365102

[51] Xiao X, Lu P, Fischer A J, Coltrin M E, Wang G T, Koleske D D and Tsao J Y 2015 Influence of pH on the Quantum-Size-Controlled Photoelectrochemical Etching of Epitaxial InGaN Quantum Dots *J. Phys. Chem. C* **119** 28194–8

[52] Zhang Y, Ryu S-W, Yerino C, Leung B, Sun Q, Song Q, Cao H and Han J 2010 A conductivity-based selective etching for next generation GaN devices *phys. stat. sol. (b)* **247** 1713–6

[53] Sailor M J 2011 Preparation of Spatially Modulated Porous Silicon Layers *Porous Silicon in Practice* (Wiley-VCH Verlag GmbH & Co. KGaA) pp 77–117

[54] Agarwal V 2014 Porous Silicon Multilayers and Superlattices *Handbook of Porous Silicon* ed L Canham (Springer International Publishing) pp 153–62

Accepted Manuscript

1
2
3
4
5
6
7
8
9
10
11
12
13
14
15
16
17
18
19
20
21
22
23
24
25
26
27
28
29
30
31
32
33
34
35
36
37
38
39
40
41
42
43
44
45
46
47
48
49
50
51
52
53
54
55
56
57
58
59
60

[55] Park J, Kang J-H and Ryu S-W 2013 High Diffuse Reflectivity of Nanoporous GaN Distributed Bragg Reflector Formed by Electrochemical Etching *Appl. Phys. Express* **6** 072201

[56] Fareed R S Q, Adivarahan V, Chen C Q, Rai S, Kuokstis E, Yang J W, Khan M A, Caissie J and Molnar R J 2004 Air-bridged lateral growth of crack-free Al0.24Ga0.76N on highly relaxed porous GaN *Appl. Phys. Lett.* **84** 696–8

[57] Huang K-P, Wu K-C, Fan F-H, Tseng W-P, Shieh B-C, Chen S-H and Lin C-F 2014 InGaN Light-Emitting Diodes with Multiple-Porous GaN Structures Fabricated through a Photoelectrochemical Etching Process *ECS J. Solid State Sci. Technol.* **3** R185–8

[58] Yuan G, Xiong K, Zhang C, Li Y and Han J 2016 Optical Engineering of Modal Gain in a III-Nitride Laser with Nanoporous GaN *ACS Photonics* **3** 1604–10

[59] Liu L, Yang C, Patanè A, Yu Z, Yan F, Wang K, Lu H, Li J and Zhao L 2017 High-detectivity ultraviolet photodetectors based on laterally mesoporous GaN *Nanoscale* **9** 8142–8

[60] Hsu W-J, Chen K-T, Huang W-C, Wu C-J, Dai J-J, Chen S-H and Lin C-F 2016 InGaN light emitting diodes with a nanopipe layer formed from the GaN epitaxial layer *Opt. Express, OE* **24** 11601–10

[61] Mishkat-Ul-Masabih S M, Luk T S, Monavarian M and Feezell D F 2019 Polarization-pinned emission of a continuous-wave optically pumped nonpolar GaN-based VCSEL using nanoporous distributed Bragg reflectors *Opt. Express, OE* **27** 9495–501

[62] Shieh B-C, Jhang Y-C, Huang K-P, Huang W-C, Dai J-J, Lai C-F and Lin C-F 2015 InGaN light-emitting diodes with embedded nanoporous GaN distributed Bragg reflectors *Appl. Phys. Express* **8** 082101

[63] Massabuau F C-P, Griffin P H, Springbett H P, Liu Y, Kumar R V, Zhu T and Oliver R A 2019 Dislocations as channels for the fabrication of sub-surface porous GaN by electrochemical etching *Under Review*

[64] Yang X, Chen Z, Cao D, Zhao C, Shen L, Luan C, Pang Z, Liu J, Ma J and Xiao H 2019 Large-area, liftoff nanoporous GaN distributed Bragg reflectors: Fabrication and application *Applied Surface Science* **489** 849–55

[65] Spiridon B F, Griffin P H, Jarman J C, Liu Y, Zhu T, Luca A D, Oliver R A and Udrea F 2018 On-Chip Thermal Insulation Using Porous GaN *Proceedings* **2** 776

[66] Trichas E, Kayambaki M, Iliopoulos E, Pelekanos N T and Savvidis P G 2009 Resonantly enhanced selective photochemical etching of GaN *Appl. Phys. Lett.* **94** 173505

[67] Lee K J, Chun J, Kim S-J, Oh S, Ha C-S, Park J-W, Lee S-J, Song J-C, Baek J H and Park S-J 2016 Enhanced optical output power of InGaN/GaN light-emitting diodes grown on a silicon (111) substrate with a nanoporous GaN layer *Opt. Express* **24** 4391–8

Accepted Manuscript

1
2
3
4
5
6
7
8
9
10
11
12
13
14
15
16
17
18
19
20
21
22
23
24
25
26
27
28
29
30
31
32
33
34
35
36
37
38
39
40
41
42
43
44
45
46
47
48
49
50
51
52
53
54
55
56
57
58
59
60

[68] Yang X, Xiao H, Cao D, Zhao C, Shen L and Ma J 2018 Fabrication, annealing, and regrowth of wafer-scale nanoporous GaN distributed Bragg reflectors *Scripta Materialia* **156** 10–3

[69] Tamboli A C, Haberer E D, Sharma R, Lee K H, Nakamura S and Hu E L 2007 Room-temperature continuous-wave lasing in GaN/InGaN microdisks *Nature Photon* **1** 61–4

[70] Abud S H, Hassan Z and Yam F K 2014 Fabrication and characterization of metal-semiconductor-metal photodetector based on porous InGaN *Mater. Chem. Phys.* **144** 86–91

[71] Radzali R, Zainal N, Yam F K and Hassan Z 2013 Nanoporous InGaN of high In composition prepared by KOH electrochemical etching *Materials Science in Semiconductor Processing* **16** 2051–7

[72] Radzali R, Hassan Z, Zainal N and Yam F K 2014 Nanoporous InGaN prepared by KOH electrochemical etching with different light sources *Microelectronic Engineering* **126** 107–12

[73] Radzali R, Hassan Z, Zainal N and Yam F K 2015 Structural and optical characteristics of porous InAlGaN prepared by photoelectrochemical etching *J. Alloy. Compd.* **622** 565–71

[74] Zhu T and Oliver R A 2012 Unintentional doping in GaN *Phys. Chem. Chem. Phys.* **14** 9558–73

[75] Griffin P, Zhu T and Oliver R 2018 Porous AlGaN-Based Ultraviolet Distributed Bragg Reflectors *Materials* **11** 1487

[76] Zhang L, Guo Y N, Yan J C, Wu Q Q, Wei X C, Wang J X and Li J M 2019 Deep ultraviolet light-emitting diodes with improved performance via nanoporous AlGaN template *Opt. Express, OE* **27** 4917–26

[77] Lu X, Li J, Su K, Ge C, Li Z, Zhan T, Wang G and Li J 2019 Performance-Enhanced 365 nm UV LEDs with Electrochemically Etched Nanoporous AlGaN Distributed Bragg Reflectors *Nanomaterials* **9** 862

[78] Bergmann M A, Enslin J, Yapparov R, Hjort F, Wickman B, Marcinkevičius S, Wernicke T, Kneissl M and Haglund Å 2019 Electrochemical etching of AlGaN for the realization of thin-film devices *Appl. Phys. Lett.* **115** 182103

[79] Chiou Y, Huang L and Lee C 2010 Photoelectrochemical Function in Gate-Recessed AlGaN/GaN Metal–Oxide–Semiconductor High-Electron-Mobility Transistors *IEEE Electron Device Letters* **31** 183–5

[80] Youtsey C, Bulman G and Adesida I 1997 Photoelectrochemical etching of GaN *MRS Online Proceedings Library Archive* **468**

[81] Usikov A, Helava H, Nikiforov A, Puzyk M, Papchenko B and Makarov Y 2016 Photoelectrochemical Corrosion of GaN/AlGaN-Based p-n Structures *American Journal of Applied Sciences* **13** 845–52

Accepted Manuscript

1
2
3
4
5
6
7
8
9
10
11
12
13
14
15
16
17
18
19
20
21
22
23
24
25
26
27
28
29
30
31
32
33
34
35
36
37
38
39
40
41
42
43
44
45
46
47
48
49
50
51
52
53
54
55
56
57
58
59
60

[82] Chuah L S, Hassan Z and Abu Hassan H 2007 Dark current characteristics of Ni contacts on porous AlGaN-based UV photodetector *J. Optoelectron. Adv. Mater.* **9** 2886–90

[83] Kim J, Kim D-U, Lee J, Jeon H, Park Y and Choi Y-S 2009 AlGaN membrane grating reflector *Appl. Phys. Lett.* **95** 021102

[84] Sharma R, Haberer E D, Meier C, Hu E L and Nakamura S 2005 Vertically oriented GaN-based air-gap distributed Bragg reflector structure fabricated using band-gap-selective photoelectrochemical etching *Appl. Phys. Lett.* **87** 051107

[85] Aharonovich I, Woolf A, Russell K J, Zhu T, Niu N, Kappers M J, Oliver R A and Hu E L 2013 Low threshold, room-temperature microdisk lasers in the blue spectral range *Appl. Phys. Lett.* **103** 021112

[86] Radzali R, Hassan Z, Zainal N and Yam F K 2015 Preparation of porous InAlGaN/Si(111) by photoelectrochemical etching for high performance hydrogen gas sensors at room temperature *Sens. Actuator B-Chem.* **213** 276–84

[87] Zhang C, ElAfandy R and Han J 2019 Distributed Bragg Reflectors for GaN-Based Vertical-Cavity Surface-Emitting Lasers *Applied Sciences* **9** 1593

[88] Butté R, Carlin J-F, Feltin E, Gonschorek M, Nicolay S, Christmann G, Simeonov D, Castiglia A, Dorsaz J, Buehlmann H J, Christopoulos S, Hög G B H von, Grundy A J D, Mosca M, Pinquier C, Py M A, Demangeot F, Frandon J, Lagoudakis P G, Baumberg J J and Grandjean N 2007 Current status of AlInN layers lattice-matched to GaN for photonics and electronics *J. Phys. D: Appl. Phys.* **40** 6328–6344

[89] Dorsaz J, Carlin J-F, Gradecak S and Ilegems M 2005 Progress in AlInN–GaN Bragg reflectors: Application to a microcavity light emitting diode *Journal of Applied Physics* **97** 084505

[90] Mishkat-Ul-Masabih S M, Aragon A A, Monavarian M, Luk T S and Feezell D F 2019 Electrically injected nonpolar GaN-based VCSELs with lattice-matched nanoporous distributed Bragg reflector mirrors *Appl. Phys. Express* **12** 036504

[91] Zhou T, Zhang C, ElAfandy R, Yuan G, Deng Z, Xiong K, Chen F-M, Kuo Y-K, Xu K and Han J 2019 Thermal transport of nanoporous gallium nitride for photonic applications *Journal of Applied Physics* **125** 155106

[92] Anderson R, Cohen D, Mehari S, Nakamura S and DenBaars S 2019 Electrical injection of a 440nm InGaN laser with lateral confinement by nanoporous-GaN *Opt. Express, OE* **27** 22764–9

[93] Griffin P H, Patel K, Zhu T, Langford R M, Kamboj V S, Ritchie D A and Oliver R A 2019 Using FIB-SEM serial block-face imaging to understand birefringence in porous GaN DBRs *In Draft*

[94] Smartt R N and Steel W H 1959 Birefringence of Quartz and Calcite *J. Opt. Soc. Am., JOSA* **49** 710–2

Accepted Manuscript

[95] Wu C-J, Wang G-J, Kao C H, Yang Z-J, Chen H, Lin Y-S, Lin C-F and Han J 2019 Photon-Recycling in Ultraviolet GaN-Based Photodiodes with Porous AlGaN Distributed Bragg Reflectors *ACS Appl. Nano Mater.* **2** 5044–8

[96] Beh K P, Yam F K, Tan L K, Ng S W, Chin C W and Hassan Z 2013 Photoelectrochemical Fabrication of Porous GaN and Their Applications in Ultraviolet and Ammonia Sensing *Jpn. J. Appl. Phys.* **52** 08JK03

[97] Peng F, Qin S-J, Hu L-F, Wang J-Y, Yang J-M, Chen X-Q and Pan G-B 2016 Electrochemical fabrication and optoelectronic properties of hybrid heterostructure of CuPc/porous GaN *Chemical Physics Letters* **652** 6–10

[98] Meng R, Ji X, Lou Z, Yang J, Zhang Y, Zhang Z, Bi W, Wang J and Wei T 2019 High-performance nanoporous-GaN metal-insulator-semiconductor ultraviolet photodetectors with a thermal oxidized Ga_2O_3 layer *Opt. Lett., OL* **44** 2197–200

[99] Zimmermann T, Neuburger M, Benkart P, Hernandez-Guillen F J, Pietzka C, Kunze M, Daumiller I, Dadgar A, Krost A and Kohn E 2006 Piezoelectric GaN sensor structures *IEEE Electron Device Letters* **27** 309–12

[100] Huang C-T, Song J, Lee W-F, Ding Y, Gao Z, Hao Y, Chen L-J and Wang Z L 2010 GaN Nanowire Arrays for High-Output Nanogenerators *J. Am. Chem. Soc.* **132** 4766–71

[101] Kang J-H, Jeong D K and Ryu S-W 2017 Transparent, Flexible Piezoelectric Nanogenerator Based on GaN Membrane Using Electrochemical Lift-Off *ACS Appl. Mater. Interfaces* **9** 10637–42

[102] Kang J-H, Jeong D K, Ha J-S, Lee J K and Ryu S-W 2017 Enhanced performance of a GaN piezoelectric nanogenerator with an embedded nanoporous layer via the suppressed carrier screening effect *Semicond. Sci. Technol.* **32** 025001

[103] Waseem A, Jeong D K, Johar M A, Kang J-H, Ha J-S, Lee J K and Ryu S-W 2018 Enhanced piezoelectric output of NiO/nanoporous GaN by suppression of internal carrier screening *Semicond. Sci. Technol.* **33** 065007

[104] Wright J S, Lim W, Norton D P, Pearton S J, Ren F, Johnson J L and Ural A 2010 Nitride and oxide semiconductor nanostructured hydrogen gas sensors *Semicond. Sci. Technol.* **25** 024002

[105] Zhang M-R, Chen X-Q and Pan G-B 2017 Electrosynthesis of gold nanoparticles/porous GaN electrode for non-enzymatic hydrogen peroxide detection *Sensors and Actuators B: Chemical* **240** 142–7

[106] Zhang M, Liu Y, Wang J and Tang J 2019 Photodeposition of palladium nanoparticles on a porous gallium nitride electrode for nonenzymatic electrochemical sensing of glucose *Microchim Acta* **186** 83

[107] Zhang M-R and Pan G-B 2017 Porous GaN electrode for anodic stripping voltammetry of silver(I) *Talanta* **165** 540–4

Accepted Manuscript

[108] Maeda K and Domen K 2010 Photocatalytic Water Splitting: Recent Progress and Future Challenges *J. Phys. Chem. Lett.* **1** 2655–61

[109] Cao D, Xiao H, Fang J, Liu J, Gao Q, Liu X and Ma J 2017 Photoelectrochemical water splitting on nanoporous GaN thin films for energy conversion under visible light *Mater. Res. Express* **4** 015019

[110] Alvi N H, Soto Rodriguez P E D, Kumar P, Gómez V J, Aseev P, Alvi A H, Alvi M A, Willander M and Nötzel R 2014 Photoelectrochemical water splitting and hydrogen generation by a spontaneously formed InGaN nanowall network *Appl. Phys. Lett.* **104** 223104

[111] Ryu S-W, Zhang Y, Leung B, Yerino C and Han J 2012 Improved photoelectrochemical water splitting efficiency of nanoporous GaN photoanode *Semicond. Sci. Technol.* **27** 015014

[112] Yang C, Xi X, Yu Z, Cao H, Li J, Lin S, Ma Z and Zhao L 2018 Light Modulation and Water Splitting Enhancement Using a Composite Porous GaN Structure *ACS Appl. Mater. Interfaces* **10** 5492–7

[113] Benton J, Bai J and Wang T 2014 Utilisation of GaN and InGaN/GaN with nanoporous structures for water splitting *Appl. Phys. Lett.* **105** 223902

[114] Chhajed S, Lee W, Cho J, Schubert E F and Kim J K 2011 Strong light extraction enhancement in GaInN light-emitting diodes by using self-organized nanoscale patterning of p-type GaN *Appl. Phys. Lett.* **98** 071102

[115] Mynbaeva M, Titkov A, Kryzhanovski A, Kotousova I, Zubrilov A S, Ratnikov V V, Davydov V Y, Kuznetsov N I, Mynbaev K, Tsvetkov D V, Stepanov S, Cherenkov A and Dmitriev V A 1999 Strain relaxation in GaN layers grown on porous GaN sublayers *Materials Research Society Internet Journal of Nitride Semiconductor Research* **4** e14

[116] Cao D, Zhao C, Yang X and Xiao H 2019 Fabrication and improved properties of InGaN-based LED with multilayer GaN/nanocavity structure *Journal of Alloys and Compounds* **806** 487–91

[117] Soh C B, Chow S Y, Tan L Y, Hartono H, Liu W and Chua S J 2008 Enhanced luminescence efficiency due to carrier localization in InGaN/GaN heterostructures grown on nanoporous GaN templates *Appl. Phys. Lett.* **93** 173107

[118] Ueda T, Ishida M and Yuri M 2011 Separation of Thin GaN from Sapphire by Laser Lift-Off Technique *Jpn. J. Appl. Phys.* **50** 041001

[119] Rajan A, Rogers D J, Ton-That C, Zhu L, Phillips M R, Sundaram S, Gautier S, Moudakir T, El-Gmili Y, Ougazzaden A, Sandana V E, Teherani F H, Bove P, Prior K A, Djebbour Z, McClintock R and Razeghi M 2016 Wafer-scale epitaxial lift-off of optoelectronic grade GaN from a GaN substrate using a sacrificial ZnO interlayer *J. Phys. D: Appl. Phys.* **49** 315105

Accepted Manuscript

[120] Zhang Y, Sun Q, Leung B, Simon J, Lee M L and Han J 2011 The fabrication of large-area, free-standing GaN by a novel nanoetching process *Nanotechnology* **22** 045603

[121] Yang X, Chen Z, Cao D, Zhao C, Shen L, Luan C, Pang Z, Liu J, Ma J and Xiao H 2019 Large-area, liftoff nanoporous GaN distributed Bragg reflectors: Fabrication and application *Applied Surface Science*

[122] Hwang D, Yonkee B P, Addin B S, Farrell R M, Nakamura S, Speck J S and DenBaars S 2016 Photoelectrochemical liftoff of LEDs grown on freestanding c-plane GaN substrates *Opt. Express, OE* **24** 22875–80

Accepted Manuscript